

T H E U N I V E R S I T Y O F M I C H I G A N

COLLEGE OF ENGINEERING
Department of Atmospheric and Oceanic Science

Technical Report

ON THE AXISYMMETRIC, STEADY STATE
STRUCTURE OF THE ATMOSPHERE

Maria R. Perez-Discerni

Aksel C. Wiin-Nielsen¹⁾

¹⁾ Present affiliation: European Centre for Medium-Range Weather Forecasts
Bracknell, U.K.

DRDA Project 002630

supported in part by:

NATIONAL SCIENCE FOUNDATION
GRANT NO. GA-16166
WASHINGTON, D.C.

administered through:

DIVISION OF RESEARCH DEVELOPMENT AND ADMINISTRATION ANN ARBOR

August 1974

TABLE OF CONTENTS

	Page
LIST OF FIGURES	iv
ABSTRACT	vi
1. INTRODUCTION	1
2. THE MODEL	2
3. SPECIFIED HEATING	6
4. NEWTONIAN HEATING	20
5. CONCLUDING REMARKS	39
6. ACKNOWLEDGMENTS	40
REFERENCES	41

LIST OF FIGURES

Figure		Page
1	The heating of an atmospheric column as a function of latitude and time. Unit: $10^{-5} \text{ kJt}^{-1} \text{ sec}^{-1}$ (Fuenzalida, 1973).	8
2	The heating for January as a function of latitude. Solid curve is the deviation H' from the average over the globe. The circles are the points obtained by summing the series of Legendre polynomials with $N=17$. Unit: $10^{-5} \text{ kJt}^{-1} \text{ sec}^{-1}$.	11
3	The computed 50 cb temperatures as a function of latitude and time. Unit: $^{\circ}\text{K}$.	13
4	The zonally averaged winds at the 75cb level as a function of latitude and time. Unit: msec^{-1} .	15
5	As Fig.4, but for 25 cb.	16
6	The zonally averaged vertical velocity as a function of latitude and time. Unit: $10^{-6} \text{ cbsec}^{-1}$.	17
7	Available potential and kinetic energy as a function of time. Unit: kJm^{-2} .	19
8	The generation of available potential energy as a function of time. Unit: Wattsm^{-2} .	21
9	As Fig.3, but for Exp.No.1.	24
10	As Fig.3, but for Exp.No.2.	25
11	As Fig.6, but for Exp.No.1.	27
12	As Fig.6, but for Exp.No.2.	28
13	As Fig.4, but for Exp.No.1.	30
14	As Fig.4, but for Exp.No.2.	31
15	As Fig.5, but for Exp.No.1.	32
16	As Fig.5, but for Exp.No.2.	33
17	As Fig.7, but for Exp.No.1.	34
18	As Fig.7, but for Exp.No.2.	36

LIST OF FIGURES (continued)

Figure		Page
19	As Fig.8, but for Exp.No.1.	37
20	As Fig.8, but for Exp.No.2.	38

ABSTRACT

The steady axisymmetrical state of the atmosphere is calculated using a quasi-geostrophic, two level model. The mechanisms of the eddy transport have not been included.

The heating function determined by Fuenzalida (1973) has been used and the circulation calculated in this way is compared with similar calculations based upon various parameterizations of the heating.

Detailed analysis using Newtonian heating with radiative considerations only and incorporating other physical processes are presented.

1. INTRODUCTION

The axially-symmetric state of the atmosphere has always played a very important role in studies of the general circulation of the atmosphere. The observed state can be obtained from atmospheric data through analysis followed by an averaging process along the latitude circles. Numerous calculations of this type have been performed as given by Lorenz (1967) and others. As pointed out by Lorenz (loc. cit.) it is of considerable interest to obtain the axially-symmetric state of the atmosphere which would exist if the eddies did not exist. It is generally assumed that such a state of the atmosphere would be unstable to disturbances, and that we therefore do not observe the symmetric state. However, in order to investigate the stability properties of the symmetric state it is necessary to be able to calculate it. This problem is very difficult to solve in the general case because it requires a detailed knowledge of the heating function for the atmosphere as a function of latitude and height and of the frictional force (dissipation) as a function of the same coordinates. Even if it were possible to specify these mechanisms in detail it would still require cumbersome calculations to determine all aspects of the symmetric state of the atmosphere in the steady state.

Realizing these difficulties it is worthwhile to explore the possibility to calculate the axially symmetric state under steady conditions in somewhat restricted cases. A study of this

kind was made by Derome and Wiin-Nielsen (1972) using a quasi-geostrophic formulation and a very simple Newtonian parameterization of the heating. The main emphasis in the study was, however, on the modifications of the symmetric part of the circulation due to the existence of atmospheric eddies which transport sensible heat and momentum. During the last couple of years there has been more realistic determinations of the atmospheric heating which would exist if the atmospheric flow were quasi-geostrophic. For details of these calculations the reader is referred to the papers by Lawniczak (1969, 1970). These studies have served as background for the simulation of the axisymmetric circulation carried out by Fuenzalida (1973) and Wiin-Nielsen and Fuenzalida (1974). An integral part of the latter studies was a rather detailed parameterization of the zonally-averaged component of the atmospheric heating in terms of those parameters which are available in a two level, quasi-geostrophic model.

As a by-product of the studies mentioned above it is therefore worthwhile to calculate the steady axisymmetrical state of the atmosphere. One of the purposes of the study is to use the heating function determined by Fuenzalida (1973). Another is to compare the circulation, calculated in this way, with similar calculations based upon various parameterizations of the heating. The basic model will again be the quasi-geostrophic, two level model, but simplified to apply to the steady state, axially

symmetric circulation. The outcome of the calculation can form the basic state for a stability study of a barotropic-baroclinic nature because the calculated circulation will have horizontal as well as vertical windshear. The results of such a study will be reported at a later time.

2. THE MODEL

The basic equations for the model are

$$\frac{\partial \zeta_*}{\partial t} + \vec{V}_* \cdot \nabla (\zeta_* + f) + \vec{V}_T \cdot \nabla \zeta_T = - \epsilon \zeta_4 \quad (2.1)$$

$$\begin{aligned} \frac{\partial \zeta_T}{\partial t} + \vec{V}_* \cdot \nabla \zeta_T + \vec{V}_T \cdot \nabla (\zeta_* + f) = \lambda^2 \left(\frac{\partial \psi_T}{\partial t} + \vec{V}_* \cdot \nabla \psi_T \right) - \lambda^2 \frac{R}{2f_0 c_p} H_2 \\ - 2A \zeta_T + \epsilon \zeta_4 \end{aligned} \quad (2.2)$$

We note that

$$\lambda^2 = \frac{2f_0^2}{\sigma P^2} \quad (2.3)$$

where f_0 is a standard value of the Coriolis parameter, $\sigma = -(\alpha/\theta)(\partial\theta/\partial p)$ a measure of static stability, α the specific volume, θ the potential temperature, p the pressure, and $P = 50$ cb. ϵ is a coefficient which is defined as follows:

$$\epsilon = \frac{g}{P} c_d \rho_4 V_4 \quad (2.4)$$

where g is the acceleration of gravity, c_d the drag coefficient, ρ the density, and V a typical value of the windspeed. In addition

$$A = \frac{g^2 \nu}{R^2 T_2^2} \quad (2.5)$$

where ν is the coefficient of viscosity, R the gas constant, and T_2 a standard value of the temperature at 50 cb. We note finally that c_p is the specific heat at constant pressure. The stream-function is denoted by ψ , vorticity by ζ , the horizontal wind by \vec{V} , the heating per unit time and unit mass by H_2 , and the subscripts * and T are defined as follows:

$$(\)_* = \frac{1}{2} [(\)_1 + (\)_3] \quad (2.6)$$

$$(\)_T = \frac{1}{2} [(\)_1 - (\)_3] \quad (2.7)$$

while the subscripts 0, 1, 2, 3, 4 refer to the 0, 25, 50, 75 and 100 cb levels. Detailed explanations for the parameterization leading to (2.4) and (2.5) can be found in Wiin-Nielsen (1972).

We shall now consider the quasi-geostrophic, axisymmetric, steady case. Because of the steady state assumption we neglect all time derivatives. The assumption that no eddies are present, combined with the quasi-geostrophic assumption, mean that all advection terms will vanish. It follows therefore that (2.1) and (2.2) reduce to the following simple equations

$$\zeta_4 = 0 \quad (2.8)$$

$$2A\zeta_T = -\lambda^2 \frac{R}{2f_0 c_p} H_2 \quad (2.9)$$

ζ_4 is formally the vorticity at 100 cb, but it represents the vorticity somewhere in the atmospheric planetary boundary layer.

Within the framework of the two level model ζ_4 is normally related to the vorticities at levels 1 and 3 through a suitable extrapolation formula. No great significance can be attached to the details of the method of extrapolation. We shall, however, in this study use an extrapolation formula which is consistent with the assumption that the temperature lapse rate is assumed to be constant and equal to 6.5°C/km (Derome and Wiin-Nielsen, 1971). We get then

$$\zeta_4 = \zeta_* - 1.6 \zeta_T = 0 \quad (2.10)$$

(2.9) can be transformed into an equation for the temperature by noting that

$$\zeta_T = \frac{1}{a^2 \cos \phi} \frac{d}{d\phi} \left[\cos \phi \frac{d\psi_T}{d\phi} \right] \quad (2.11)$$

and

$$\psi_T = \frac{R}{2f_0} \cdot T_2 \quad (2.12)$$

The new form of (2.9) is then

$$\frac{A}{a^2} \frac{1}{\cos \phi} \frac{d}{d\phi} \left[\cos \phi \frac{dT_2}{d\phi} \right] = - \frac{\lambda^2}{2c_p} H_2 \quad (2.13)$$

or, with $\mu = \sin \phi$

$$\frac{d}{d\mu} \left[(1 - \mu^2) \frac{dT_2}{d\mu} \right] = - \beta H_2 \quad (2.14)$$

where

$$\beta = \frac{\lambda^2 a^2}{2Ac_p} \quad (2.15)$$

If we are able to specify the heating H_2 we can solve (2.14) by suitable methods for $T_2 = T_2(\phi)$. ψ_T can then be obtained from (2.12), ψ_* from the equivalent equation to (2.10), i.e.

$$\psi_* = 1.6 \psi_T \quad (2.16)$$

and u_* and u_T can be calculated from the formulas

$$u_* = - \frac{1}{a} (1 - \mu^2)^{1/2} \frac{\partial \psi_*}{\partial \mu} \quad (2.17)$$

and

$$u_T = - \frac{1}{a} (1 - \mu^2)^{1/2} \frac{\partial \psi_T}{\partial \mu} \quad (2.18)$$

The vertical velocity ω_2 can be obtained from the steady state form of the thermodynamic equation

$$\omega_2 = - \frac{R}{c_p} \frac{1}{\sigma P} H_2 \quad (2.19)$$

If desired one can finally obtain the mean meridional velocity component v_T from the continuity equation

$$\frac{1}{a \cos \phi} \frac{\partial v_T \cos \phi}{\partial \phi} + \frac{\omega_2}{P} = 0 \quad (2.20)$$

3. SPECIFIED HEATING

One calculation of the heating function H_2 , well suited for the present model, is the estimate provided by Fuenzalida (1973). The reader is referred to this paper for details of the

various processes which was carried out from climatological information for each month of the year. Figure 1 shows the heating as a function of latitude and time of the year. These data were used as the values of H_2 in (2.14) which was then solved for T_2 in each of the 12 cases.

A few words should be said about the heating data. The original calculation was carried for each 10 degrees of latitude for the northern and southern hemisphere separately. This procedure resulted in general in two different values at the Equator. These values were averaged to obtain a unique value at $\phi=0$. For computational purposes it was furthermore needed to have the data for each 5 degrees of latitude. Interpolation was carried out using a four point interpolation formula which is based on a forward and backward use followed by averaging of Lagrange's three point interpolation formula. The final formula is best described by considering a point M in which we want the interpolated value. Denoting the values in the four surrounding points by $f(-2)$, $f(-1)$, $f(1)$ and $f(2)$ the formula is

$$f(M) = -\frac{1}{16} f(-2) + \frac{9}{16} f(-1) + \frac{9}{16} f(1) - \frac{1}{16} f(2) \quad (3.1)$$

The solution of (2.14) can be obtained in a number of ways. The most natural way is to use an expansion in Legendre functions. Suppose that H_2 is represented by the series

$$H_2 = \sum_{n=0}^N A_n P_n(\mu) \quad (3.2)$$

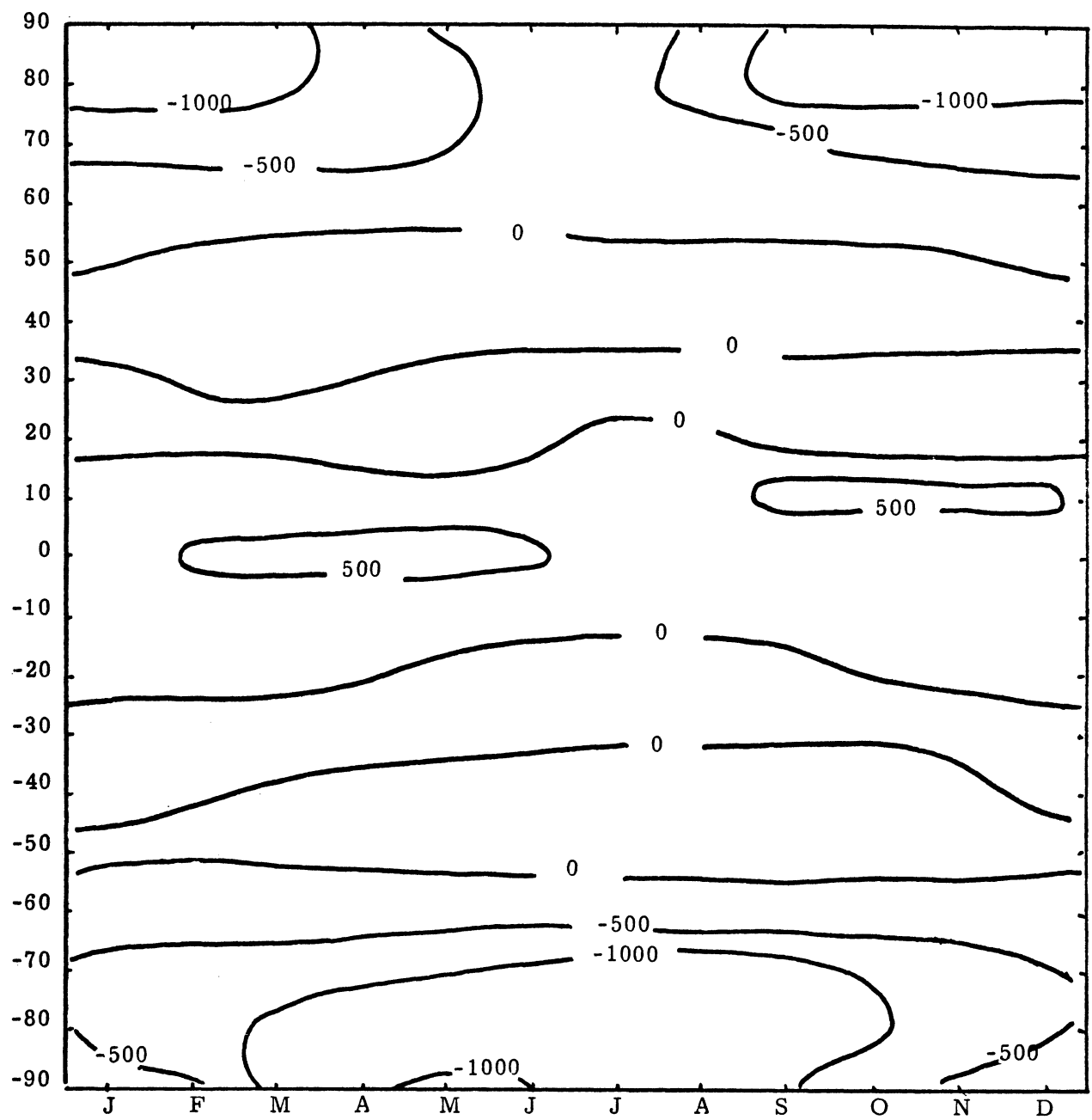


Figure 1: The heating of an atmospheric column as a function of latitude and time. Unit: $10^{-5} \text{ kJt}^{-1}\text{sec}^{-1}$ (Fuenzalida, 1973).

where A_n can be computed from the known field H_2 by the formula

$$A_n = \frac{\int_{-1}^{+1} H_2(\mu) P_n(\mu) d\mu}{\int_{-1}^{+1} P_n(\mu)^2 d\mu} \quad (3.3)$$

We know of course that

$$\int_{-1}^{+1} P_n(\mu)^2 d\mu = \frac{2}{2n+1} \quad (3.4)$$

Let the unknown temperature field be represented by

$$T_2 = \sum_{n=0}^N B_n P_n(\mu) \quad (3.5)$$

where the coefficients B_n are unknown. Substituting (3.2) and (3.5) in (2.14) and using that the functions P_n satisfy the equation

$$\frac{d}{d\mu} \left[(1 - \mu^2) \frac{dP_n}{d\mu} \right] + n(n+1)P_n = 0 \quad (3.6)$$

we find that

$$B_n = \beta \frac{A_n}{n(n+1)}, \quad n \neq 0 \quad (3.7)$$

B_0 , the global average of T_2 , cannot be determined by this procedure as can be seen from (2.14), which gives

$$\int_{-1}^{+1} H_2 d\mu = 0 \quad (3.8)$$

when integrated from the south pole to the north pole, i.e. from -1 to +1. If (3.8) is not satisfied by the empirically computed function H_2 , it is necessary to correct the original data by subtracting the average over the globe.

The values of A_n were computed from (3.3) using the 37 data points (every 5 degrees from -90° to $+90^\circ$) with $N = 17$ which gives a reasonably accurate representation of H_2 . The calculation was based on a quadrature scheme using the Neumann weights W_K which will make the Legendre functions orthogonal in the numerical integrations. This procedure is to be preferred over the simple quadrature schemes based on Newton's or Simpson's integration formulas which fail to satisfy the orthogonality condition. An example of the accuracy of the numerical scheme with $N = 17$ is shown in Figure 2 which shows the heating field, H_2' i.e. the deviation from the mean values for the month of January where the circles show values of H_2' computed by summing the series (3.2) using the computed values of A_n .

A solution of (2.14) can naturally also be obtained by finite difference methods. Such calculations were also performed because this procedure gave an opportunity to test the heuristic boundary conditions derived by Fuenzalida (1973). It is obvious that boundary conditions at the north and south pole are needed to solve (2.14) by finite differences. The proposed conditions are $dT/d\phi = 0$ at $\phi = \pm \pi/2$. Having these conditions it is straightforward to design a numerical procedure for the solution of T_2 by forming the finite difference equation using central differences

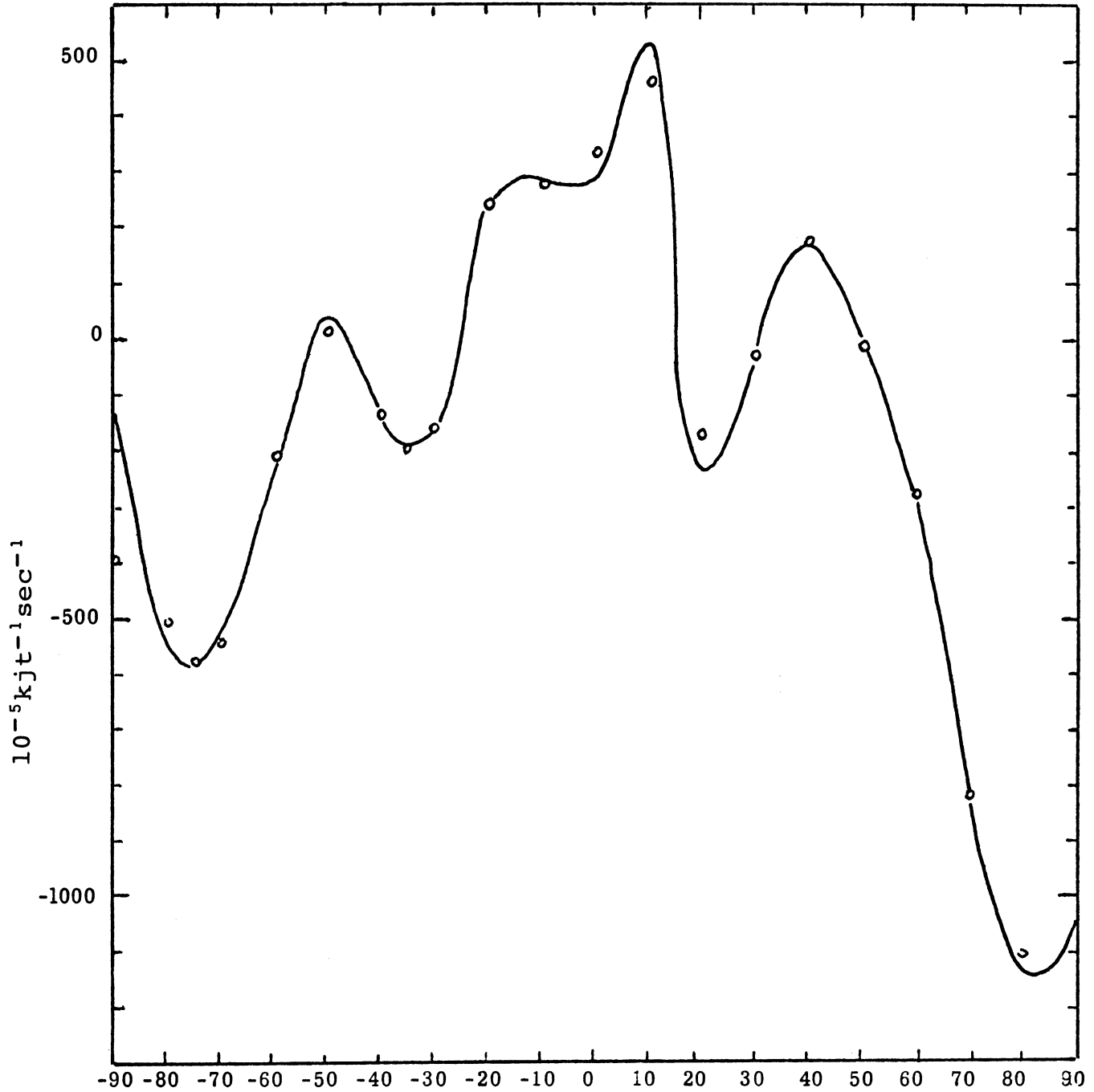


Figure 2: The heating for January as a function of latitude. Solid curve is the deviation H' from the average over the globe. The circles are the points obtained by summing the series of Legendre polynomials with $N=17$. Unit: $10^{-5} \text{ kjt}^{-1} \text{ sec}^{-1}$.

in each point and transforming these equations to a simple matrix equation which is solved by standard methods. In addition to the boundary condition $dT_2/d\phi = 0$ at $\phi = \pm \pi/2$ it is also necessary to supply one temperature. It is most convenient to introduce a fixed temperature at a certain point, say the north pole. Using this procedure we can naturally not expect to get the same absolute values as in the first method in which a series expansion in Legendre functions is used. Apart from the difference in the mean value it turns out that the finite difference method gives the same variation of $T_2 = T_2(\mu)$ in spite of the approximate conditions at $\phi = \pm \pi/2$. If the prefixed temperature at $\phi = \pi/2$ is T_* , it turns out that the best way to apply the mathematical boundary condition in the finite difference form is to use $T(90) = T(85) = T_*$ at $\phi = \pi/2$ and $T(-90) = T(-85)$ at $\phi = -\pi/2$.

We shall next describe the results of the calculation. Figure 3 shows the temperature T_2 , computed by solving (2.14) using H_2 from Fuenzalida's (1973) calculation, as a function of latitude and time of the year. The global mean value assigned to this calculation was 252°K. The temperature difference between equator and pole is very large in the calculation amounting to approximately 175°K in winter and 80°K in summer in the northern hemisphere and even larger differences in the southern hemisphere. The calculated temperature gradients are much larger than observed in the atmosphere. Since a mean

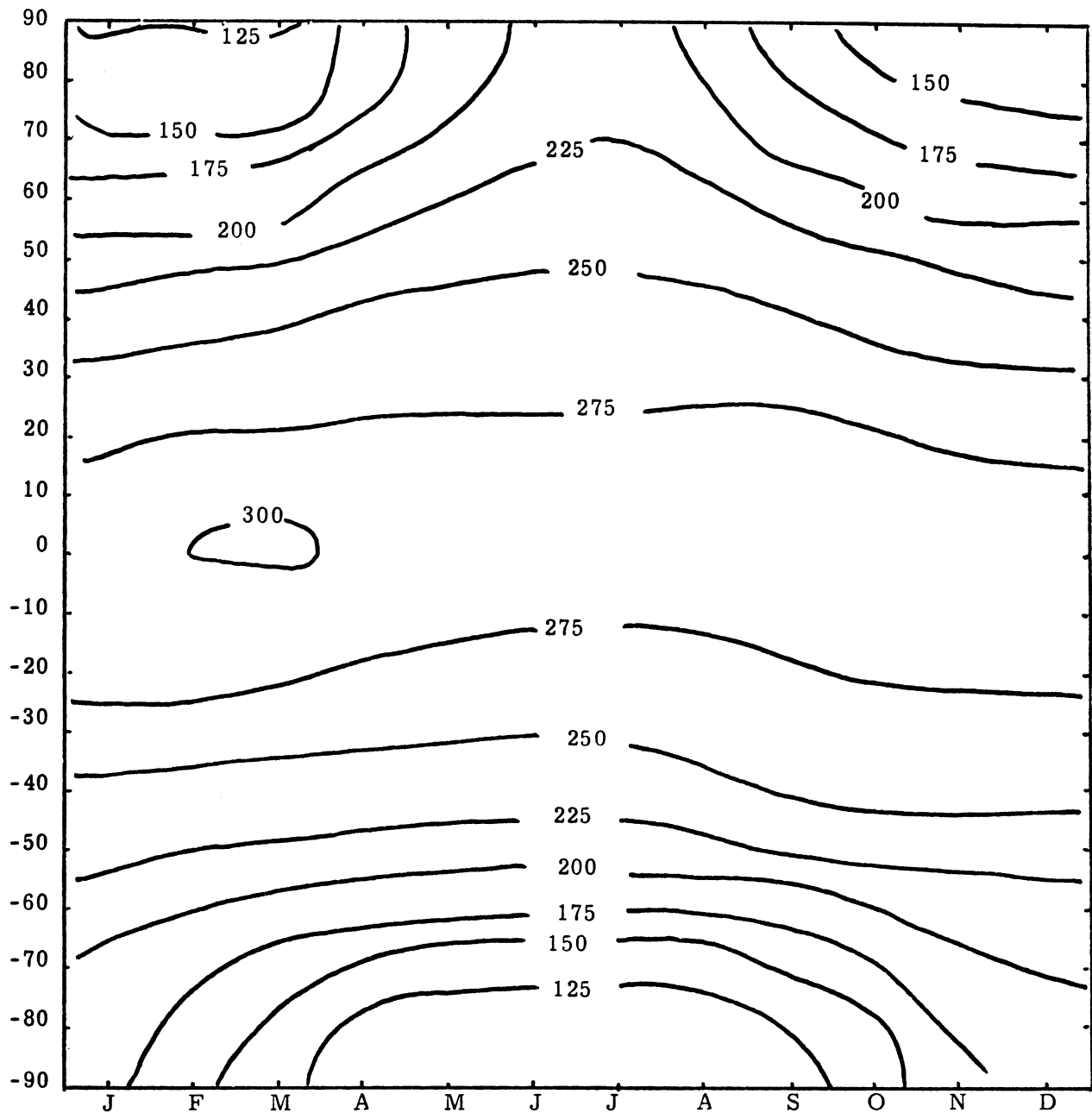


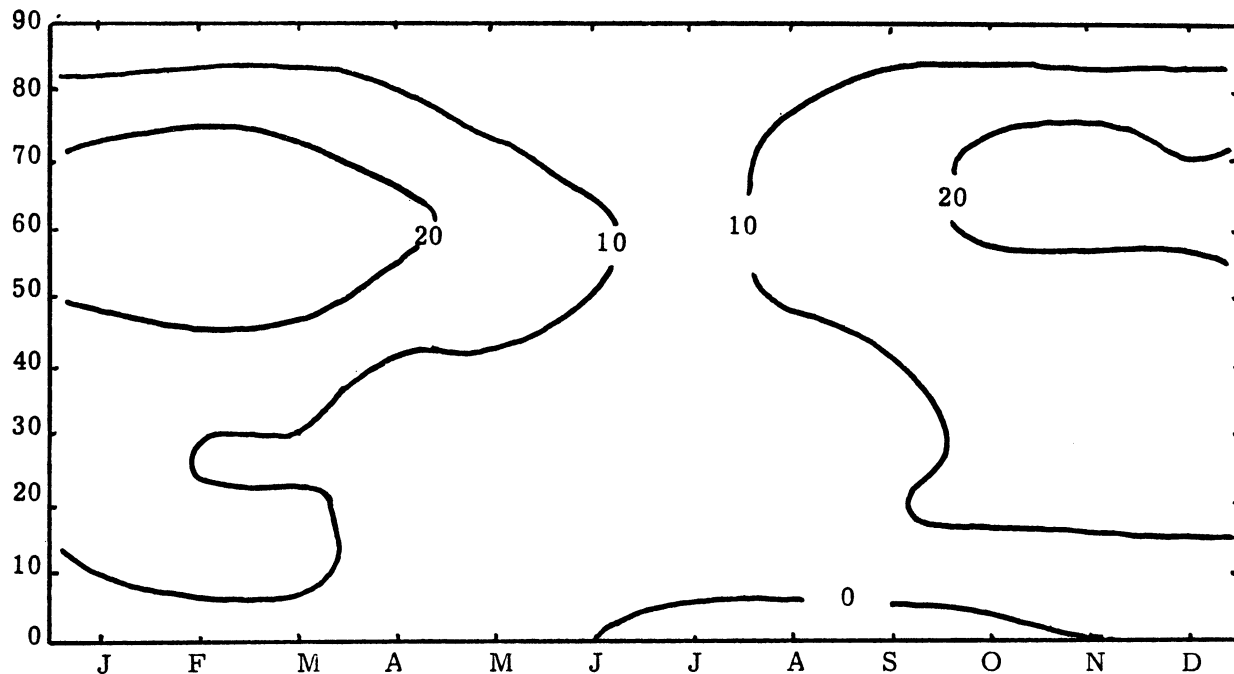
Figure 3: The computed 50 cb temperatures as a function of latitude and time. Unit:°K.

meridional circulation is included in the present model it is obvious that this circulation is unable to transport the necessary amount of heat to obtain agreement between the calculated and observed temperatures. We may therefore conclude that the required heat transport is carried out in the real atmosphere by mechanisms not included in the present model (eddies). We observe furthermore that the largest temperature gradient is located around 60°N in the northern hemisphere winter and around 60°S in the southern hemisphere winter. It is therefore found that the geostrophic thermal wind must be largest at these places calling for a jet stream at much higher latitudes than its location in the real atmosphere.

These features are found in Figures 4 and 5 which show the zonal wind distributions at the 75 and 25 cb levels, respectively. We note in particular that the winds at the upper level exceed 100 msec^{-1} in each hemisphere during the winter season of that hemisphere. Apart from the excessive windspeeds it is observed that the maximum winds are found after the winter solstice in both hemispheres. As with the temperature distribution we must again conclude that an important mechanism influencing the distribution of the zonal winds is missing in the axisymmetric model.

Figure 6 shows the zonally averaged vertical velocity as a function of latitude and time. As seen from (2.19) the vertical velocity is directly proportional to the heating in this steady state, axially symmetric model. The main information in

Northern Hemisphere



Southern Hemisphere

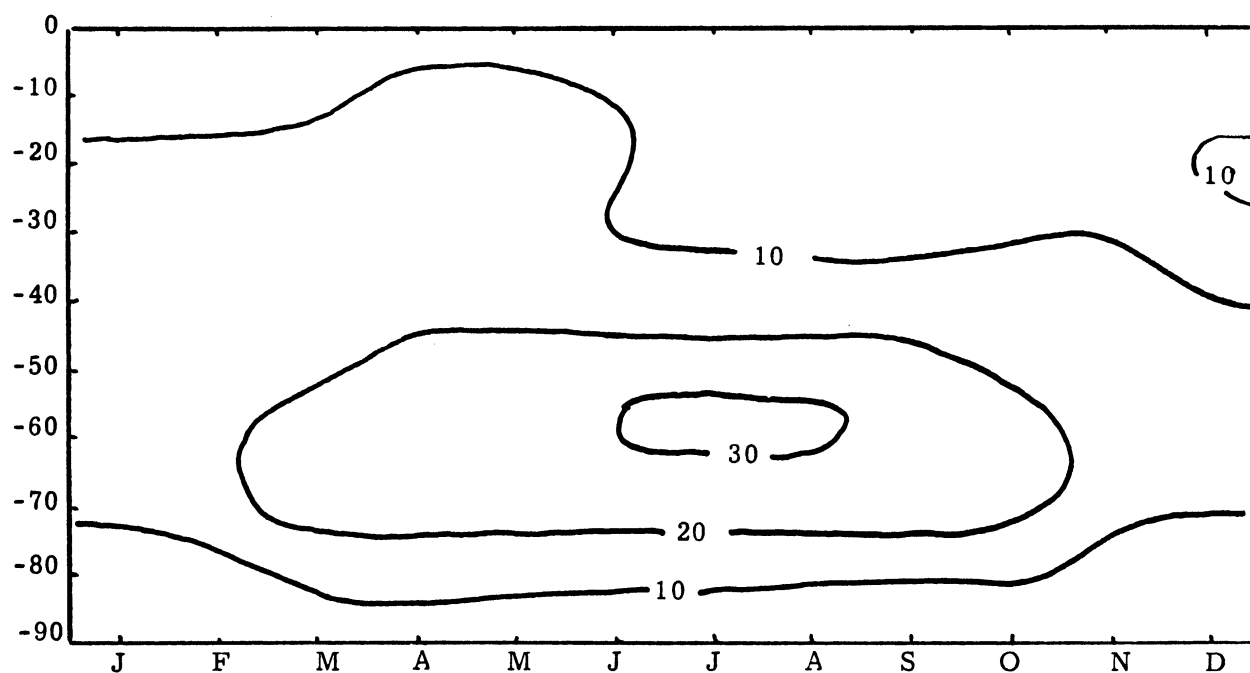
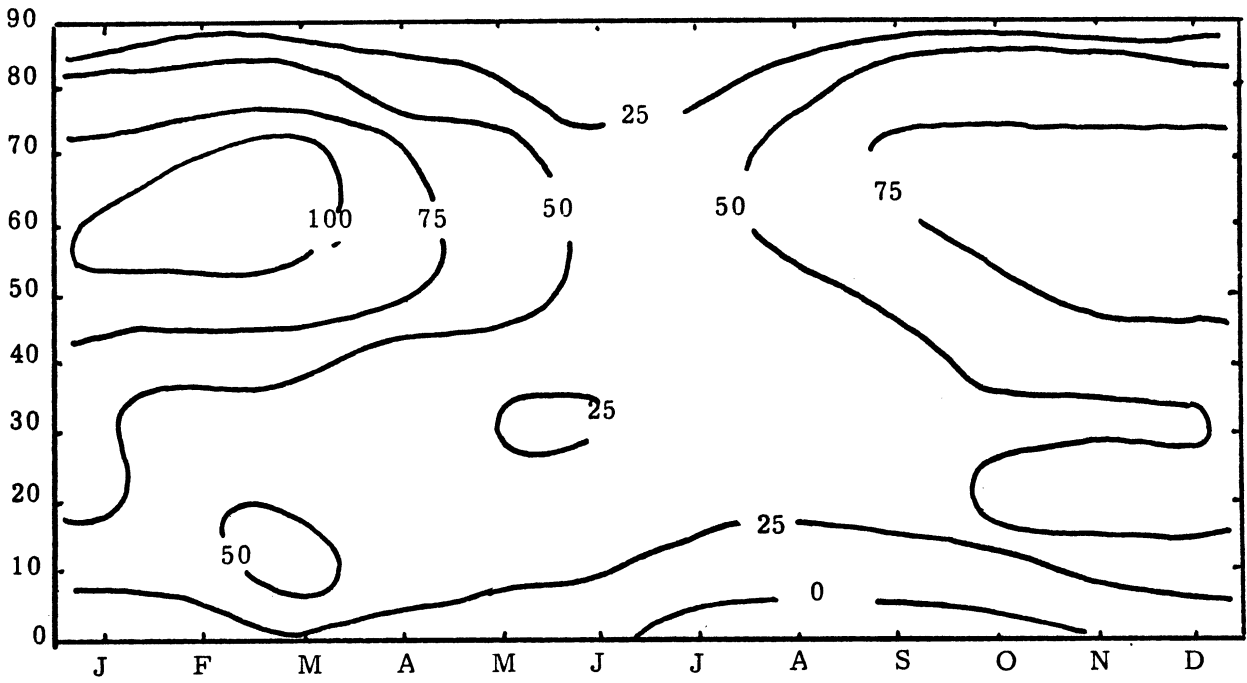


Figure 4: The zonally averaged winds at the 75 cb level as a function of latitude and time. Unit: ms⁻¹.

Northern Hemisphere



Southern Hemisphere

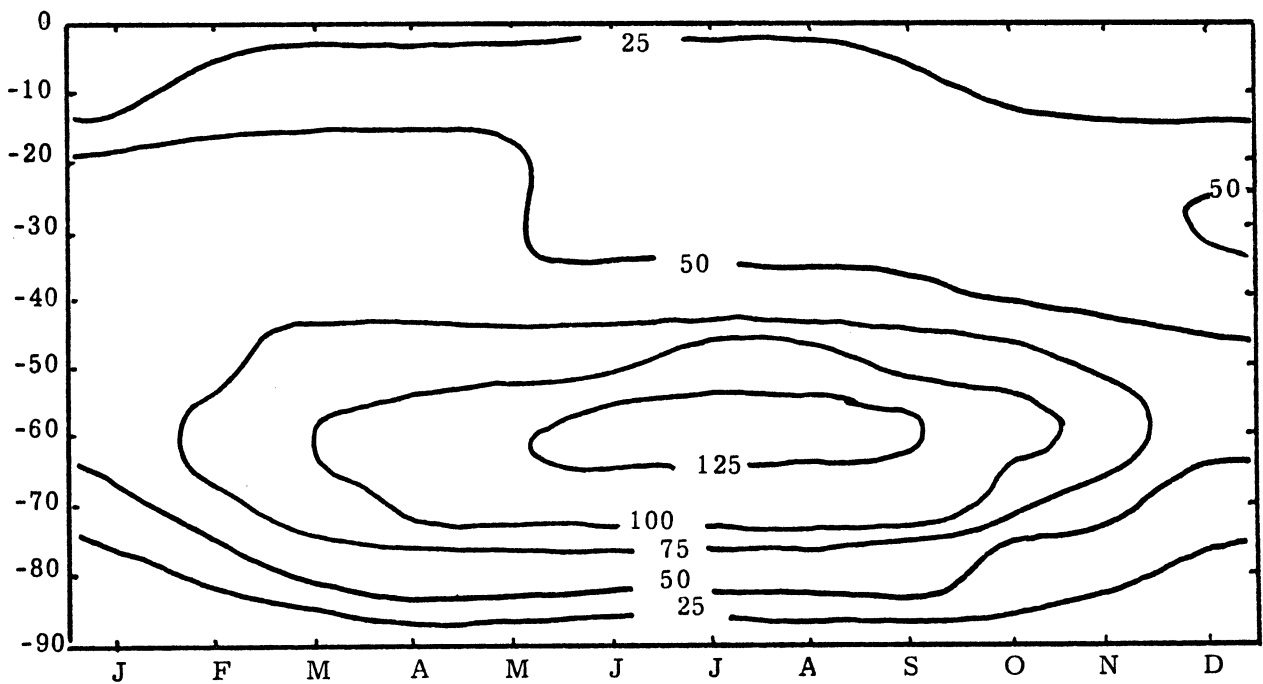


Figure 5: As Fig.4, but for 25 cb.

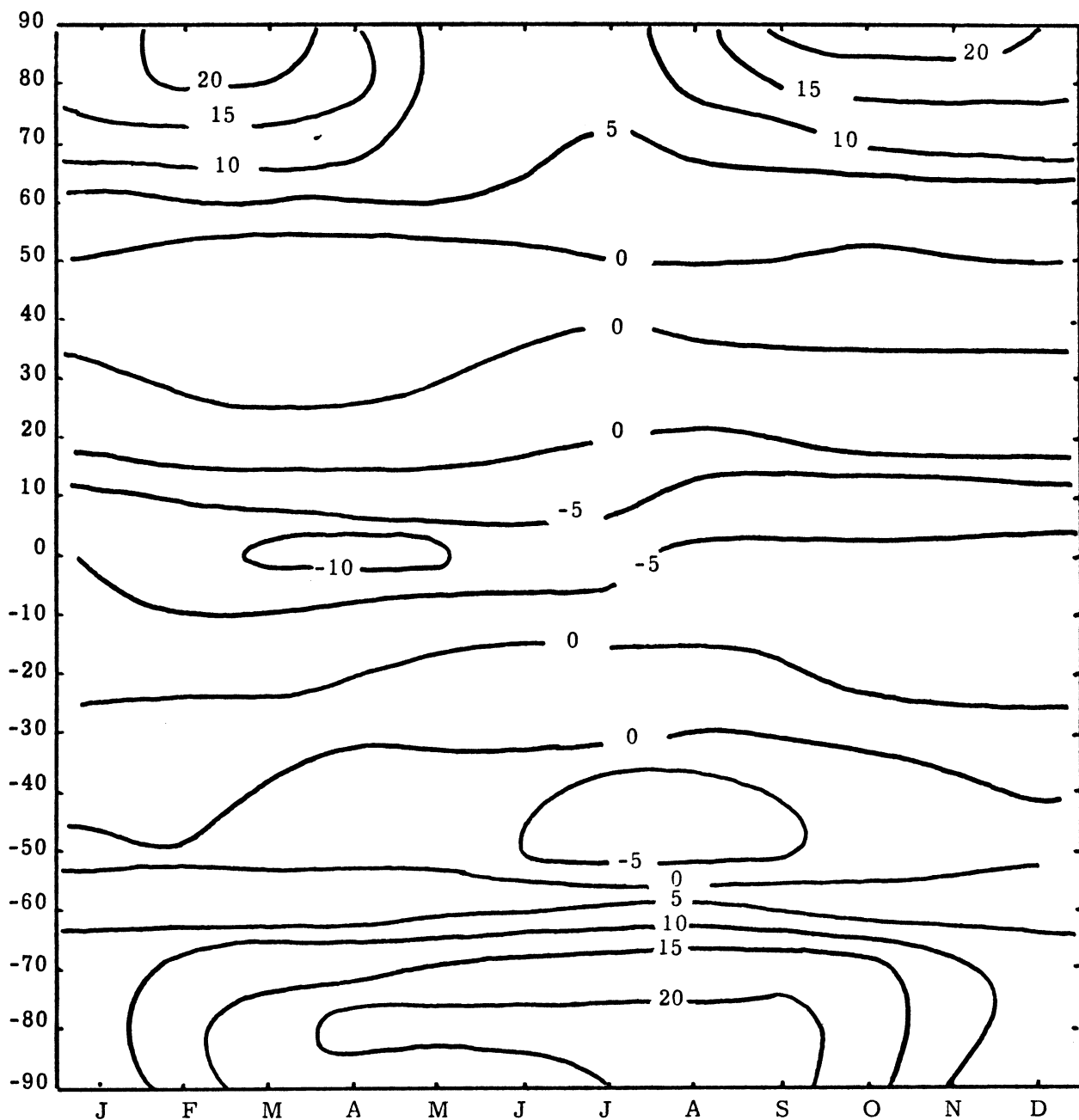
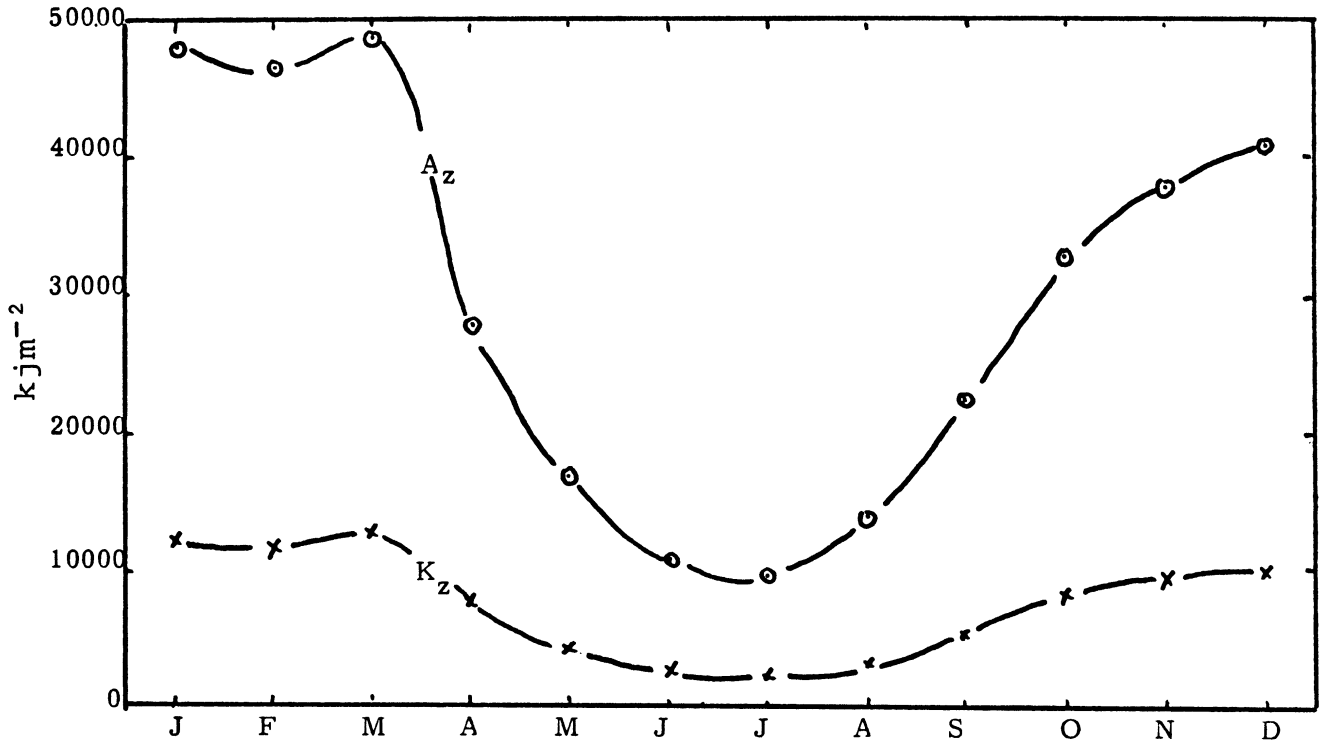


Figure 6: The zonally averaged vertical velocity as a function of latitude and time. Unit: 10^{-6} cbsec $^{-1}$.

Figure 6 is therefore the order of magnitude of the mean meridional circulation. The largest value of ω_2 is 20×10^{-6} cb sec^{-1} which corresponds to about 1.5 mmsec^{-1} . It is thus seen that the mean meridional circulation has a weak three cell pattern because such a pattern exists in the heating function as seen from Figure 1. A much simpler heating function would naturally give a correspondingly simple mean meridional circulation.

We shall next consider the energetics of the axially symmetric model. The formulas needed to compute the amounts of energy and the generations, conversions and dissipations are given in many places, but can for example be found in Wiin-Nielsen (1970). As with the other parameters we calculate the energetics as a series of steady state, and we have for convenience put the results together as a function of time during the year. Figure 7 shows the amounts of available potential energy A_z and of kinetic energy K_z separately for the northern and southern hemisphere. It is seen that A_z and K_z during the winter season attain levels many times larger than in the real atmosphere. For A_z it is naturally a reflection of the large temperature variance in the axisymmetric state due to the large temperature difference between the poles and the Equator. The large energy level for K_z is of course mainly due to the excessive windspeeds at the upper level of the model which in turn reflects the large temperature gradients in middle latitudes. In addition to these features it

Northern Hemisphere



Southern Hemisphere

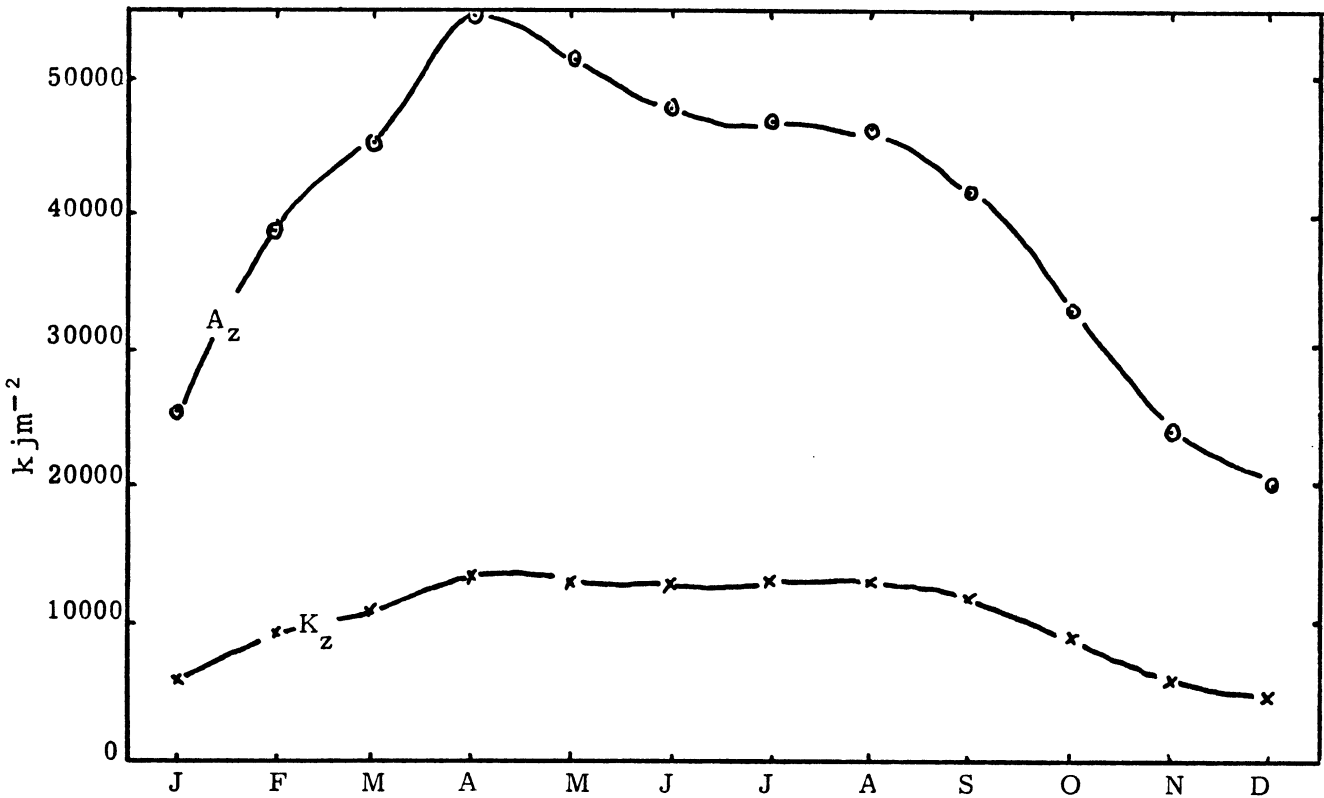


Figure 7: Available potential and kinetic energy as a function of time. Unit: kJm^{-2} .

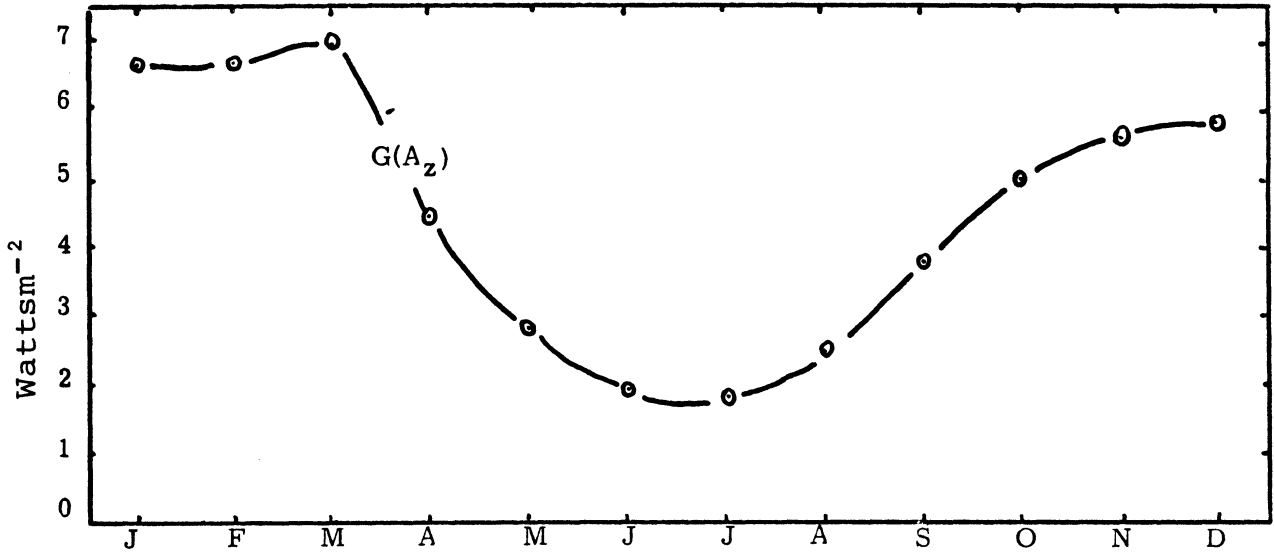
is seen that the axially symmetric calculation gives an erroneous picture of the annual variation as compared with observed state because the maxima for the northern hemisphere appear as late as the month of March.

Figure 8 shows finally that the generation of available potential energy in the axisymmetrical state would be quite large with maximum values up to about 7 Wm^{-2} during the winter season and minimum values of $2-3 \text{ Wm}^{-2}$ in the summer season. It is natural that the generation of A_z must be large in order to maintain the high energy level of A_z . Since the annual variation is computed as a succession of steady states it is obvious that the conversion from A_z to K_z , and the dissipation of K_z , is identical to the generation of A_z . It can be concluded from these calculations that the eddies in the large-scale atmospheric circulation plays a most important role in reducing the energy levels to the observed levels and at the same time decreases the intensity of the general circulation as measured by the generation of A_z .

4. NEWTONIAN HEATING

The form of Newtonian heating has been used extensively in simulations of various aspects of the general circulation. The authors have made extensive use of this formulation and generalized it in certain aspects in order to incorporate other physical processes than radiation, Wiin-Nielsen (1972). In the formulation of the more general heating mechanisms it is still

Northern Hemisphere



Southern Hemisphere

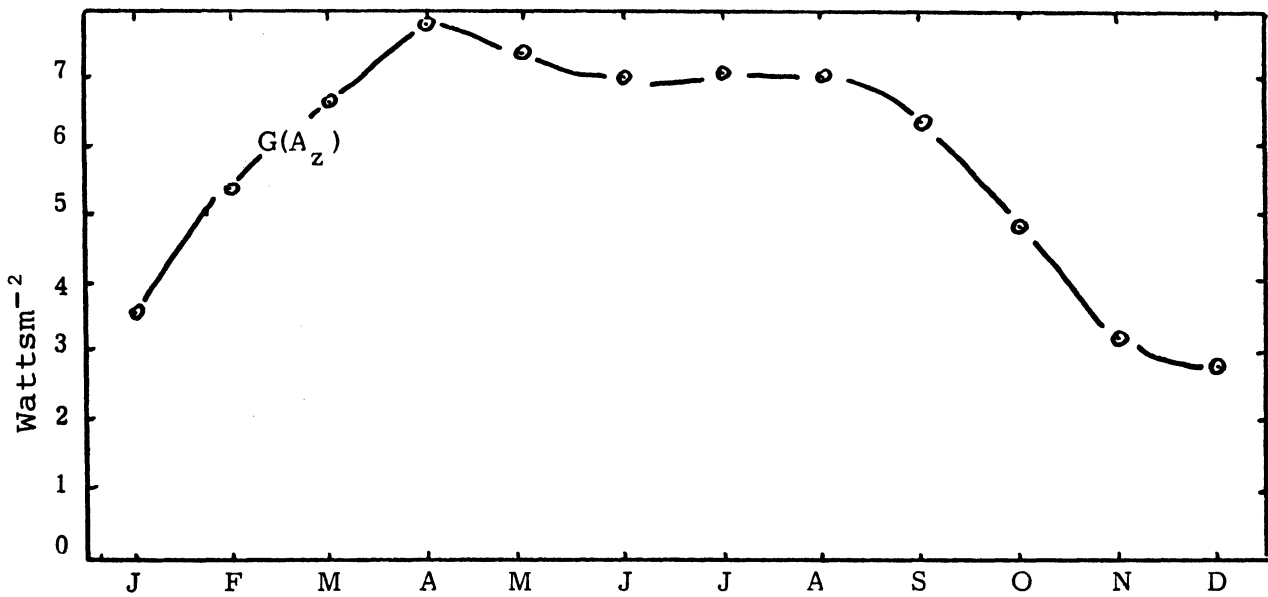


Figure 8: The generation of available potential energy as a function of time. Unit: Wattsm⁻².

possible to formulate an equilibrium temperature as shown in appendix 2 of Wiin-Nielsen (loc. cit.) although a linearization of Boltzman's law is required. Even in the most general of the considered cases it is possible to write the heating in the form

$$H_2 = - \gamma c_p (T_2 - T_E) \quad (4.1)$$

but it must be remembered that T_E and γ vary from one formulation of the heating to another. Based upon the various formulations given by Wiin-Nielsen (loc. cit.) the field of T_E was computed as a function of time and latitude. For each formulation γ was also calculated. This information was then used to solve (2.14) with H_2 replaced by (4.1) and to make the subsequent calculations of all the remaining parameters. It is seen that (2.14) takes a modified form when (4.1) is introduced because it becomes

$$\frac{d}{d\mu} \left[(1 - \mu^2) \frac{dT_2}{d\mu} \right] - \Gamma T_2 = - \Gamma T_E \quad (4.2)$$

where

$$\Gamma = \frac{\lambda^2 a^2}{2A} \gamma \quad (4.3)$$

(4.2) can again be solved using either Legendre polynomials or finite differences. In the first case there is a modification in (3.7) which becomes

$$B_n = \frac{\Gamma}{n(n+1) + \Gamma} A_n \quad (4.4)$$

Note that $B_0 = A_0$ for $n = 0$. It was found that a good representation of T_E was obtained using $N = 16$ in the equivalent of (3.2) using the Neumann weights as before. The reconstructed field has less than 1°K difference from the given field in general. A slightly larger difference, i.e. a little larger than 1°K , is found in March and October at the poles.

The equation (4.2) was also solved by finite differences using an ordinary central finite difference scheme with the boundary condition $dT_2/d\phi = 0$. The solutions of (4.2) using the two methods differ by less than 1°K with the same exception as before.

It is perhaps most instructive to consider two extreme cases. The first case is one in which the equilibrium temperature and the coefficient γ is determined by radiative considerations only, corresponding to case no. 1 of Wiin-Nielsen (1972). The other case is case no. 9 of the same paper including all the mechanisms under consideration and therefore the most general case. The results of these two cases will be presented and compared in the following paragraphs. Figures 9 and 10 show the temperature fields computed in the two cases. As expected we find that the very large temperature difference in the winter season created by radiative processes (Fig. 9) is significantly reduced by the other processes (Fig. 10). The major factor responsible for the reduction of the pole-equator difference in the winter season is the role played by the upper layer of the ocean

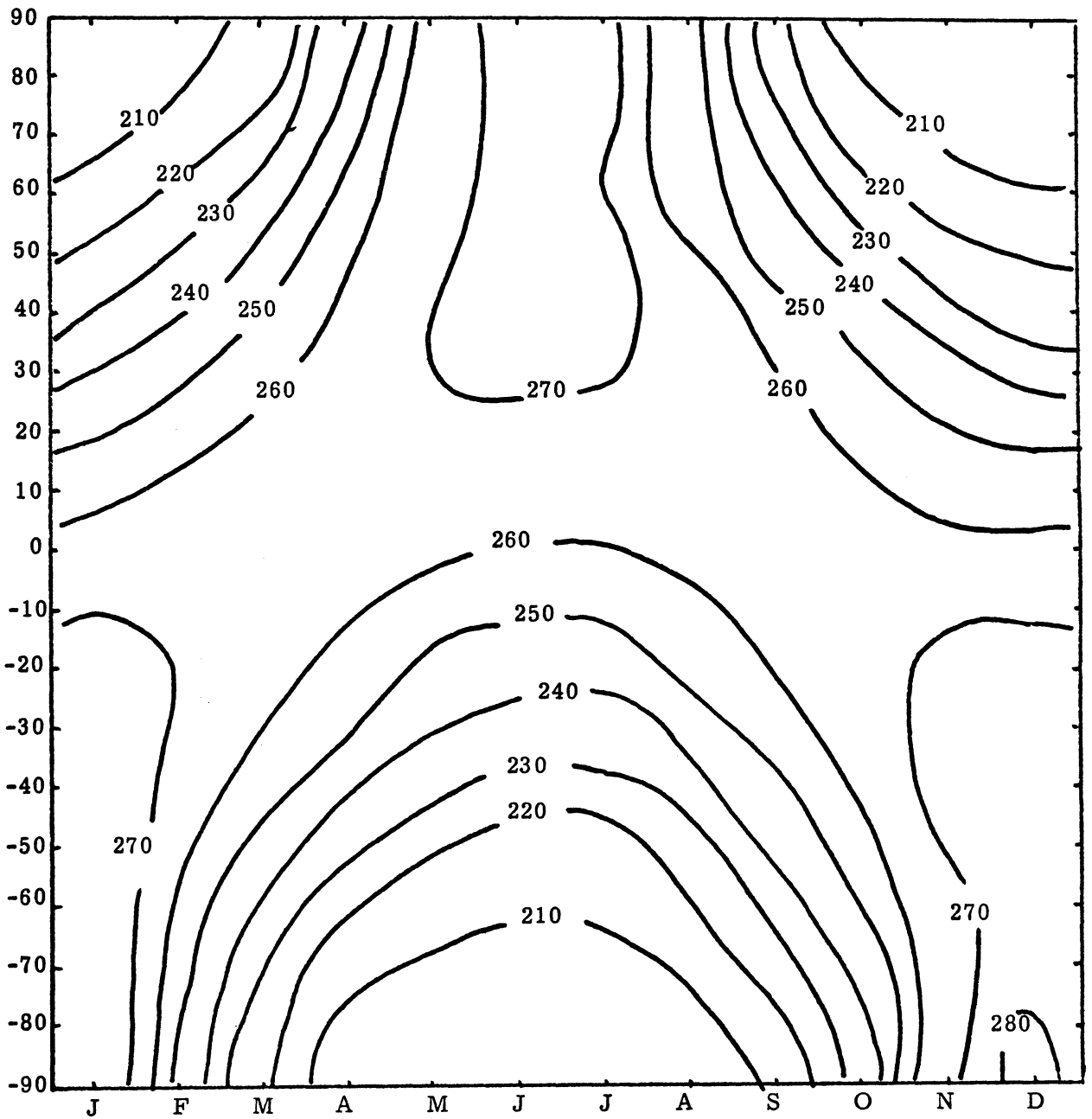


Figure 9: As Fig.3, but for Exp.No.1.

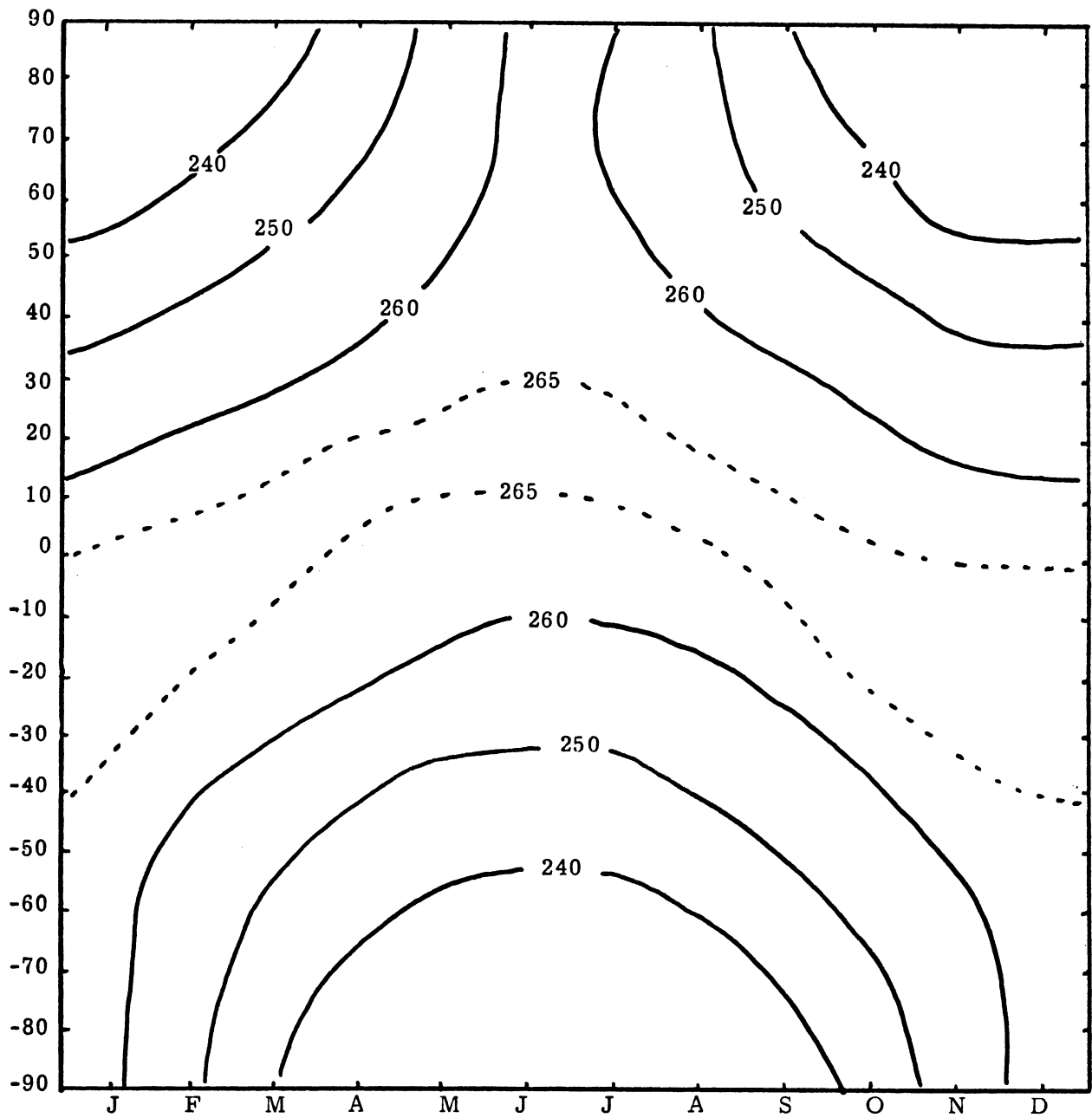


Figure 10: As Fig.3, but for Exp.No.2.

as can be seen from calculations which include radiation and conduction only, but exclude some small-scale convection and evaporation-condensation processes. The latter calculations are not displayed here but they give relatively minor modifications of the temperature field shown in Figure 10. Another important difference between Figure 9 and Figure 10 is the reversal of the temperature gradient in the summer season. In Figure 9 there is a larger temperature at the pole than at the Equator giving a decrease of the wind with height during the summer in both hemispheres. The influence of the other processes contributing to Figure 10 reverse the temperature difference and thereby create an increase of the wind with height even during the summer.

Figures 11 and 12 show the mean meridional vertical velocity for the two experiments as a function of time and latitude. Because the vertical velocity and the heating are proportional to each other, see (2.19), it is unnecessary to reproduce the heating fields for the two experiments. We note that the vertical velocity consists of a single, thermally direct, Hadley cell during the winter season with relatively weak rising motion in the low latitudes and a somewhat stronger sinking motion in the high latitudes. The cell is stronger in the first experiment than in the second indicating again the modifying influence of the other physical processes, in particular the upper layer of the ocean as the intermediate calculations (not displayed) show. The more complicated structure

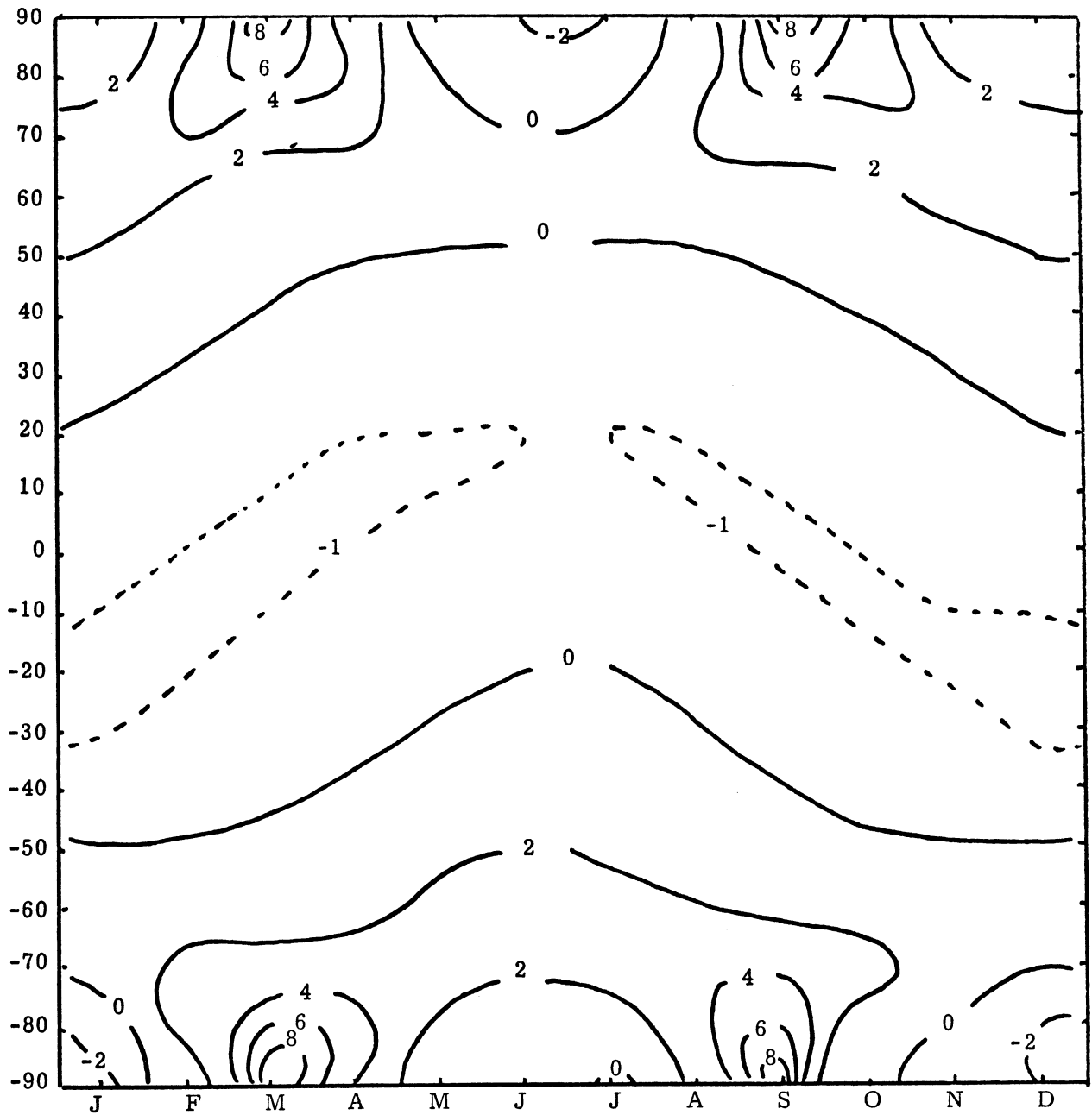


Figure 11: As Fig.6, but for Exp.No.1.

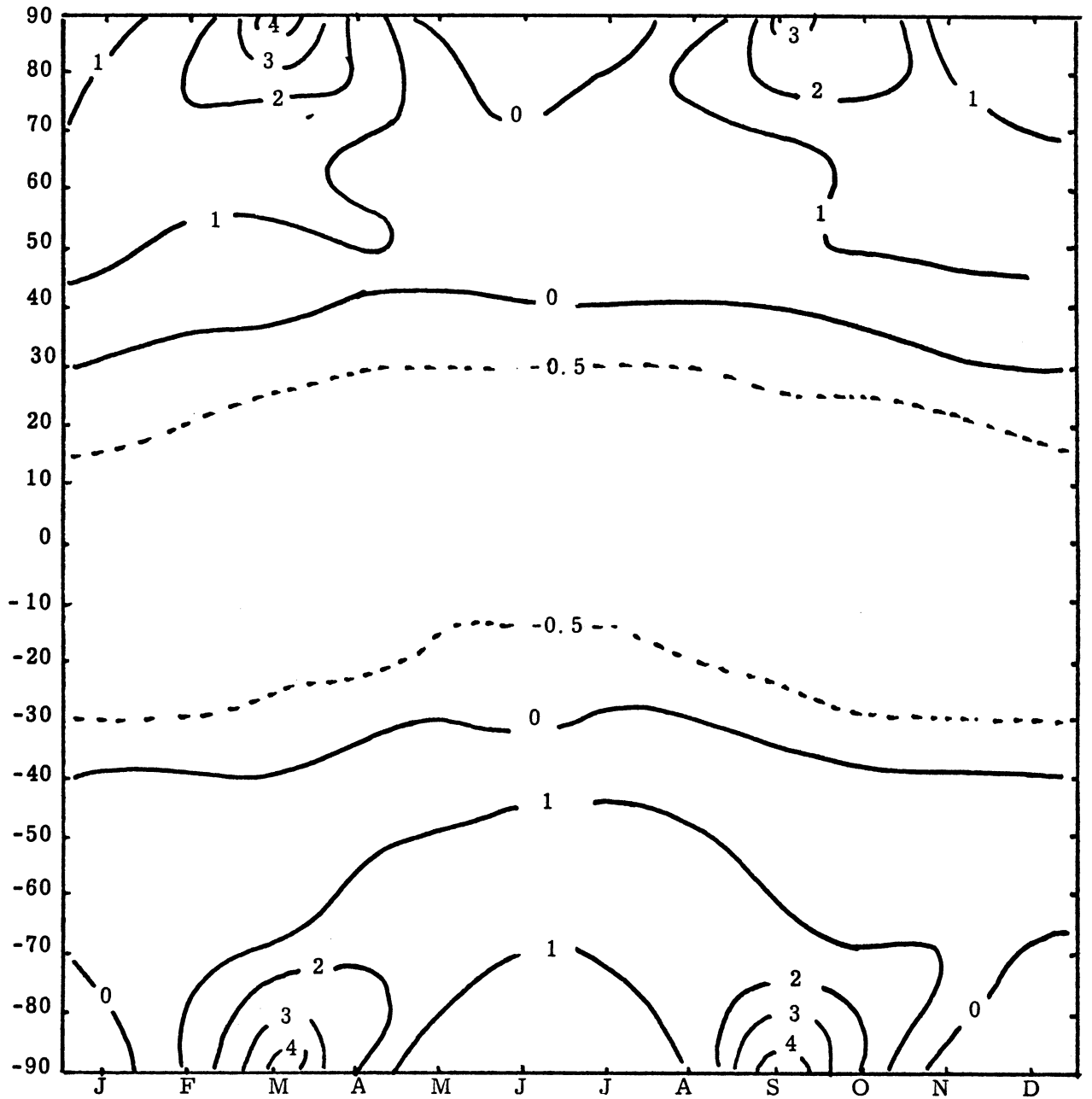


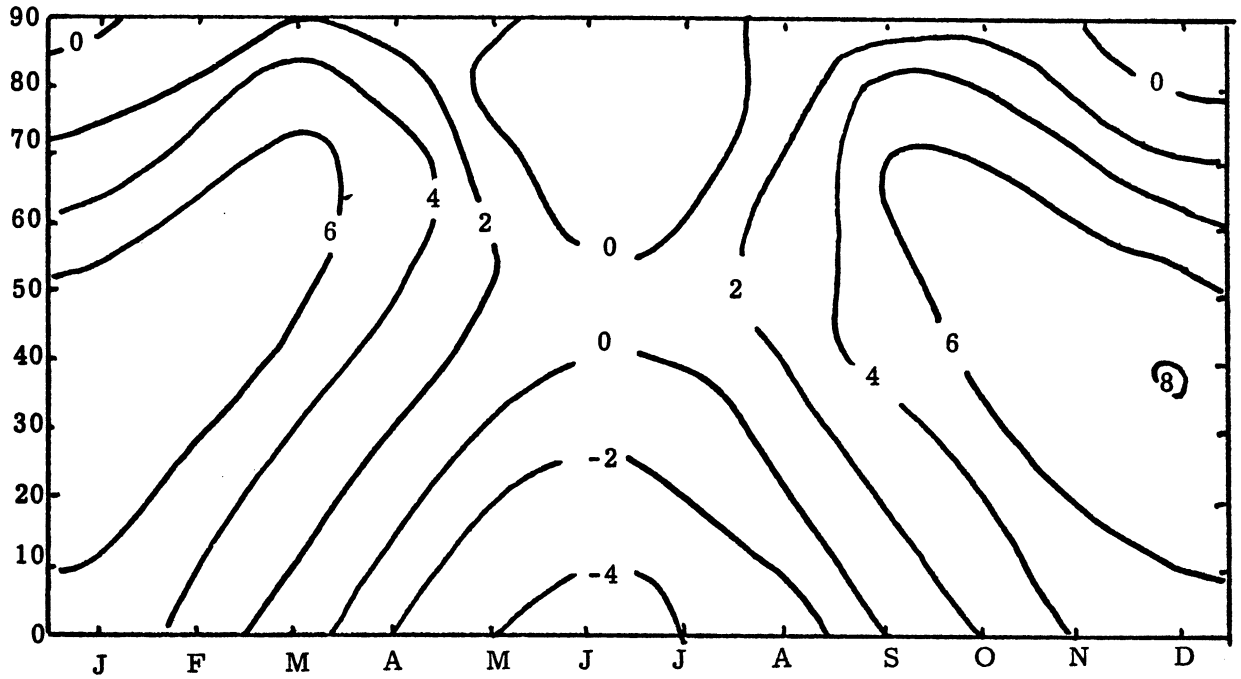
Figure 12: As Fig.6, but for Exp.No.2.

in the first experiment with two cells of which the polar cell shows rising motion during the summer over the poles has almost disappeared in the second experiment (Figure 12).

The zonal winds at the lower level (75 cb) in the first experiment are shown in Figure 13. There are westerlies during the winter season, and the maximum of the westerlies moves gradually towards the pole during spring. During summer there are easterlies almost everywhere, but westerlies of some strength appear again during the fall with a maximum at high latitudes. Gradually this maximum moves equatorward during the fall and early winter. A significant change is created by the physical processes other than radiation as seen in Figure 14 which shows the zonal winds at the lower level in the second experiment. The position of the maximum still move poleward from winter to summer, but the latitudinal displacement is now much smaller. In addition, there is now a much broader band of westerlies during the summer season in both hemispheres. The features found at the lower level can also be seen at the higher level (25 cb) for which the zonal winds are shown in Figures 15 and 16 for the two experiments, respectively. The difference is very marked in the strength of the jetstream which is about twice as strong in the first experiment (radiation) as in the second.

We shall finally consider certain aspects of the energetics of the two experiments. Figure 17 shows the annual variation of the zonal available potential energy A_z and the zonal kinetic energy K_z for the first experiment. It is seen that

Northern Hemisphere



Southern Hemisphere

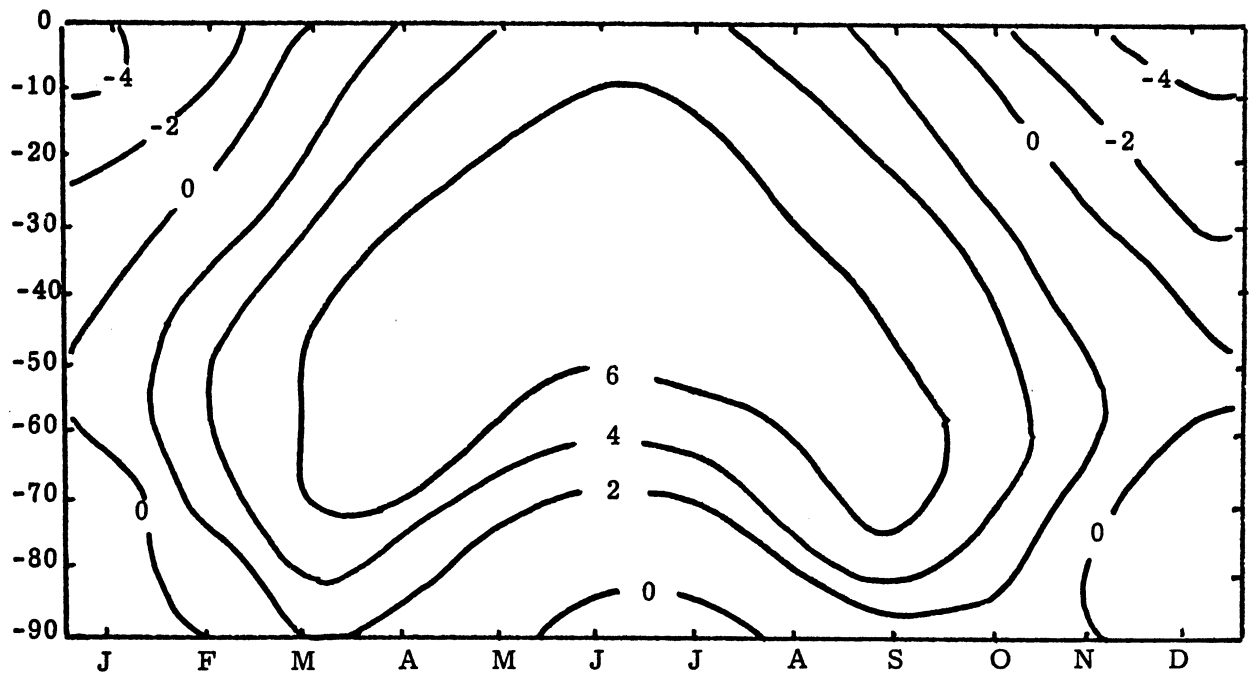
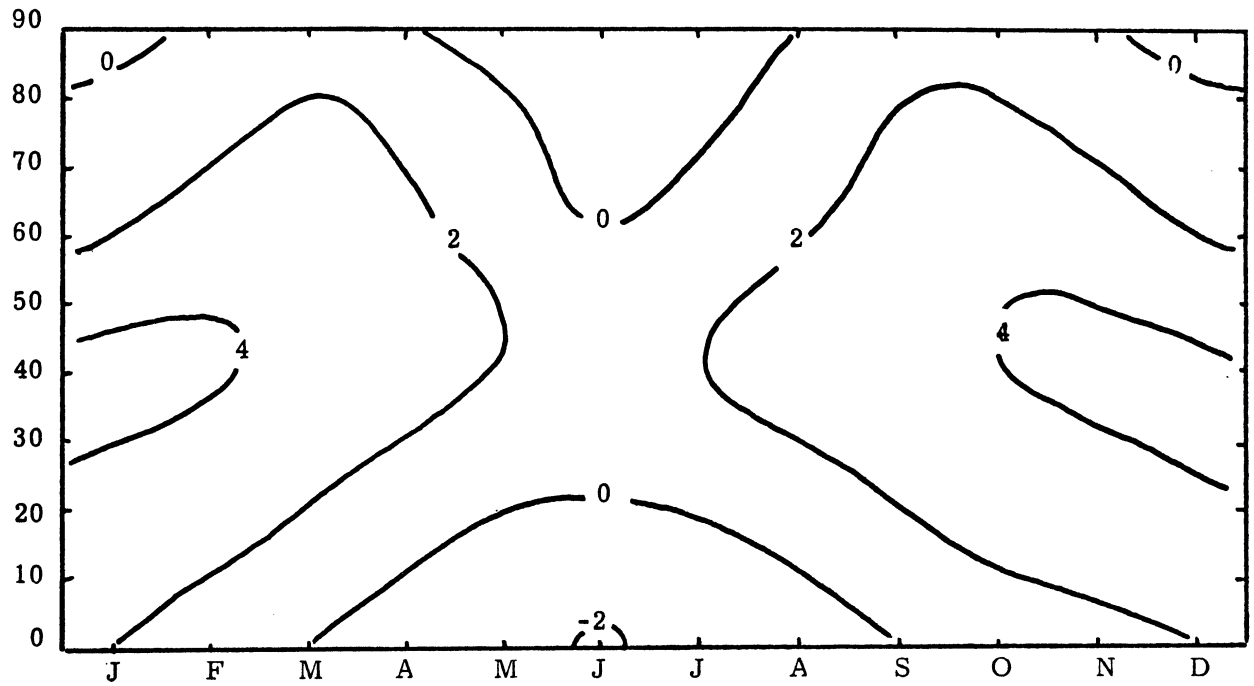


Figure 13: As Fig.4, but for Exp.No.1.

Northern Hemisphere



Southern Hemisphere

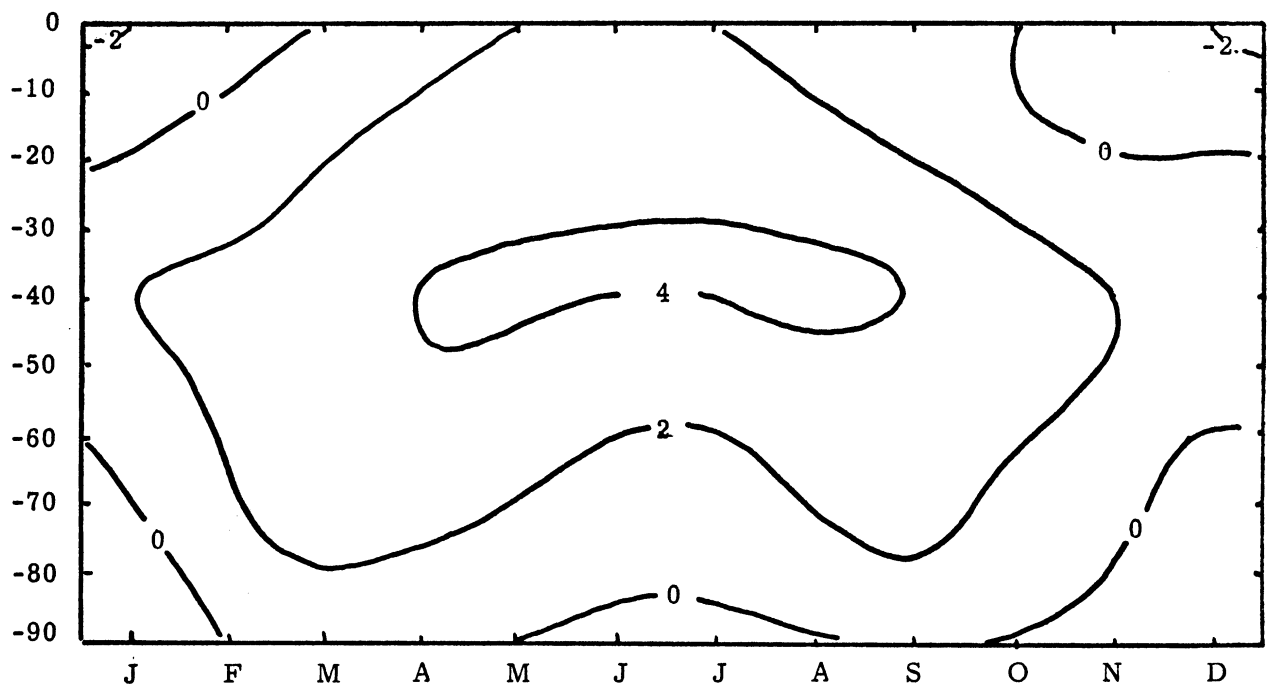
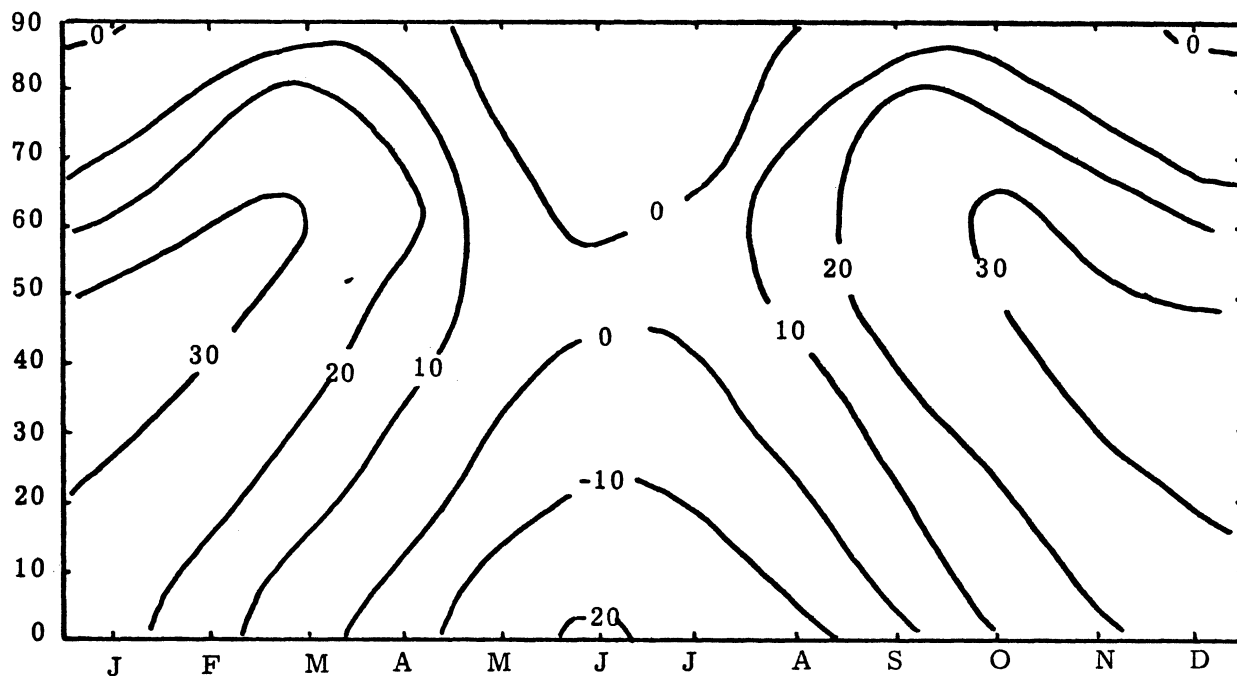


Figure 14: As Fig.4, but for Exp.No.2.

Northern Hemisphere



Southern Hemisphere

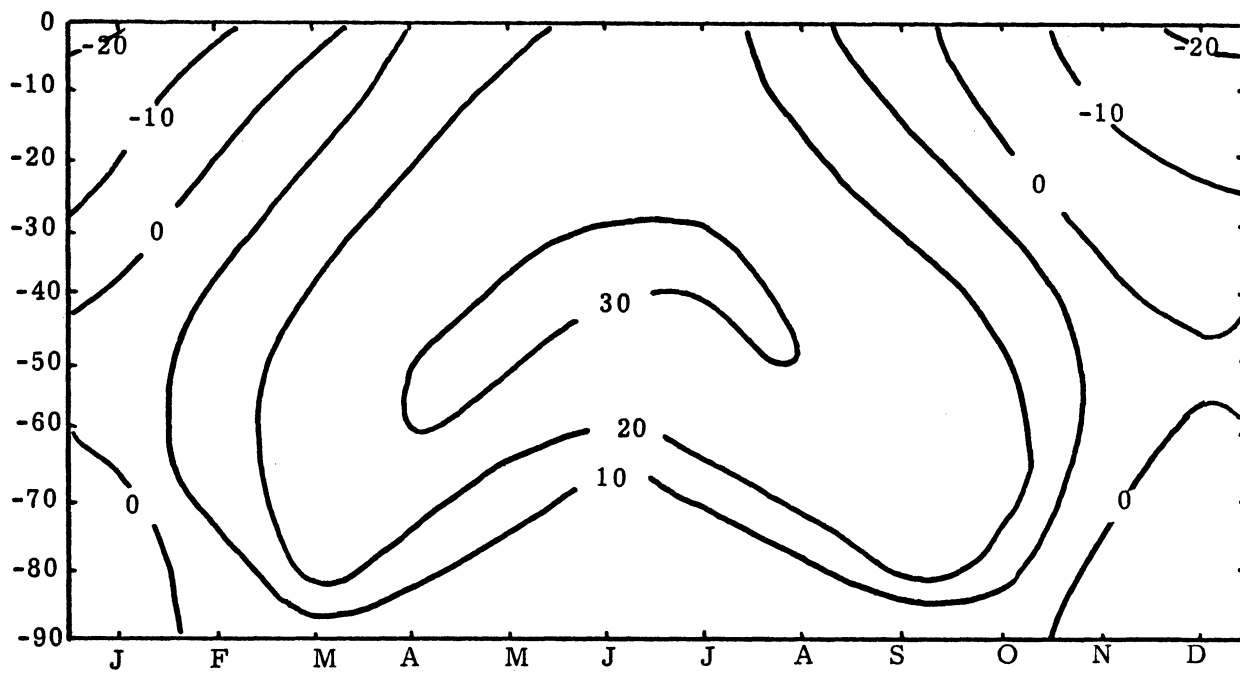
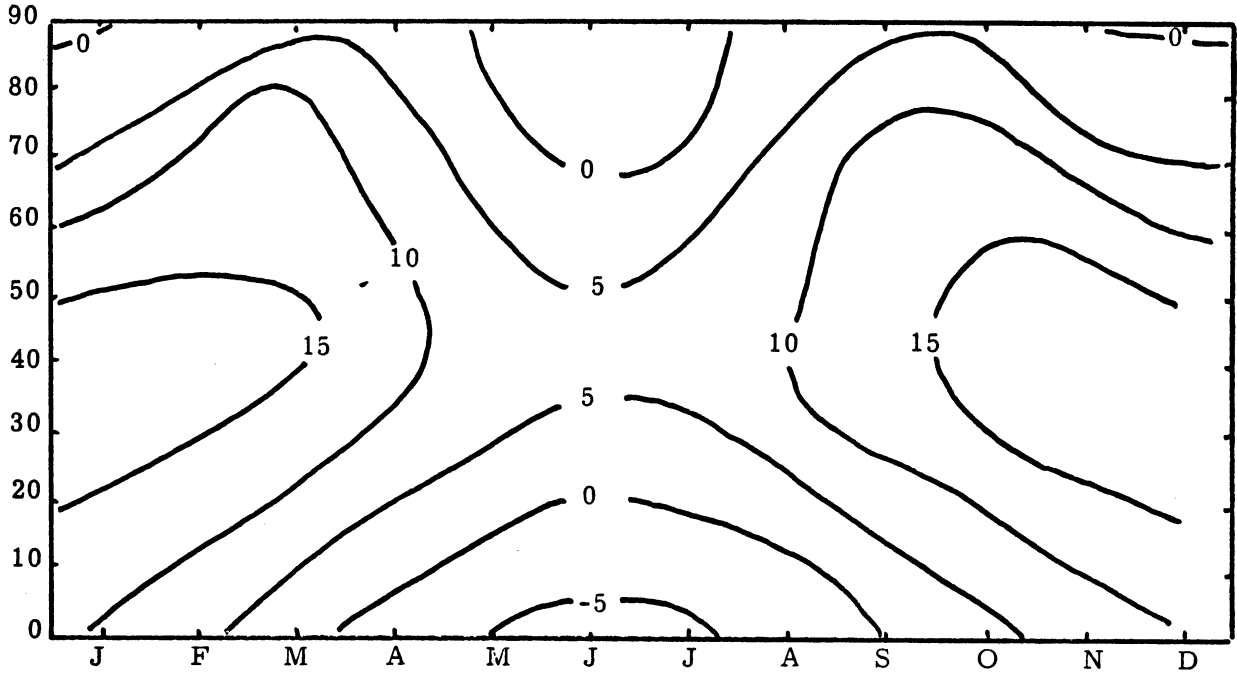


Figure 15: As Fig.5, but for Exp.No.1.

Northern Hemisphere



Southern Hemisphere

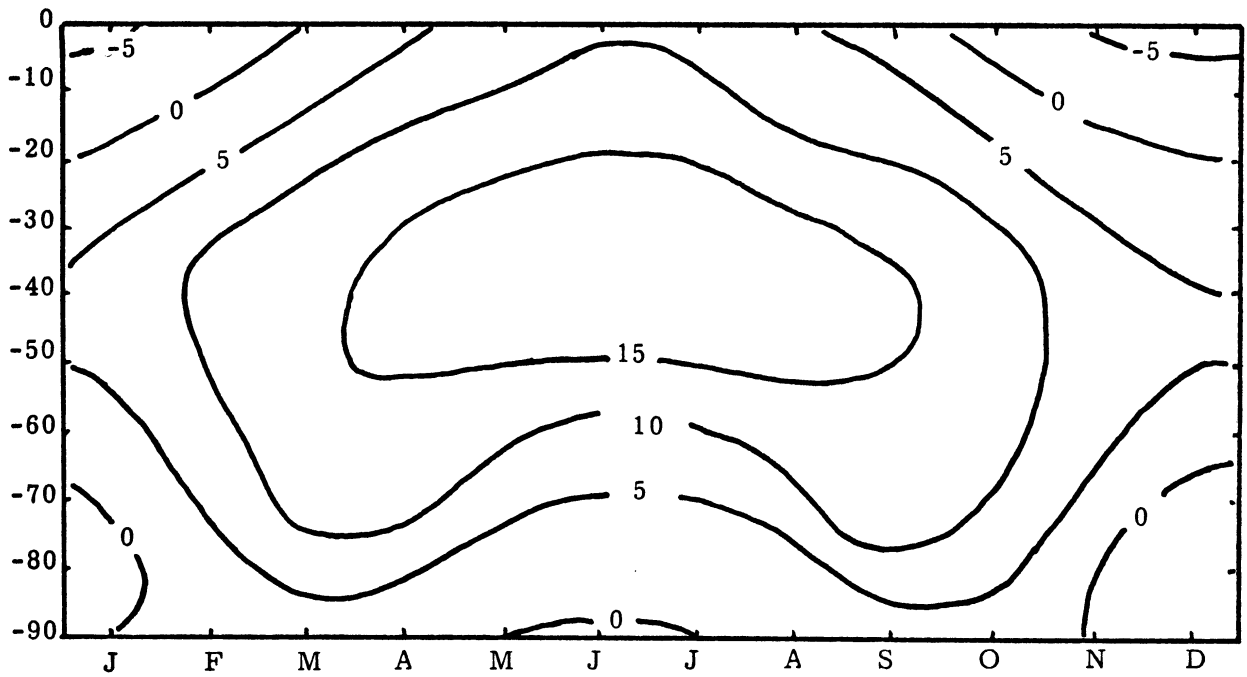
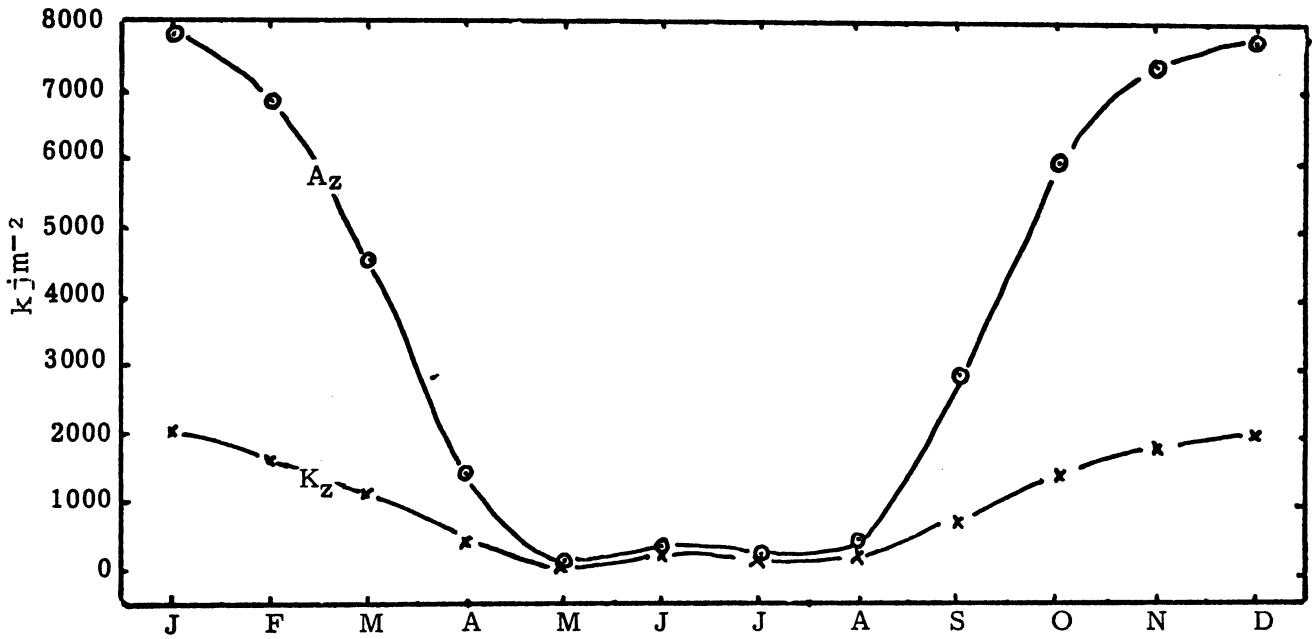


Figure 16: As Fig.5, but for Exp.No.2.

Northern Hemisphere



Southern Hemisphere

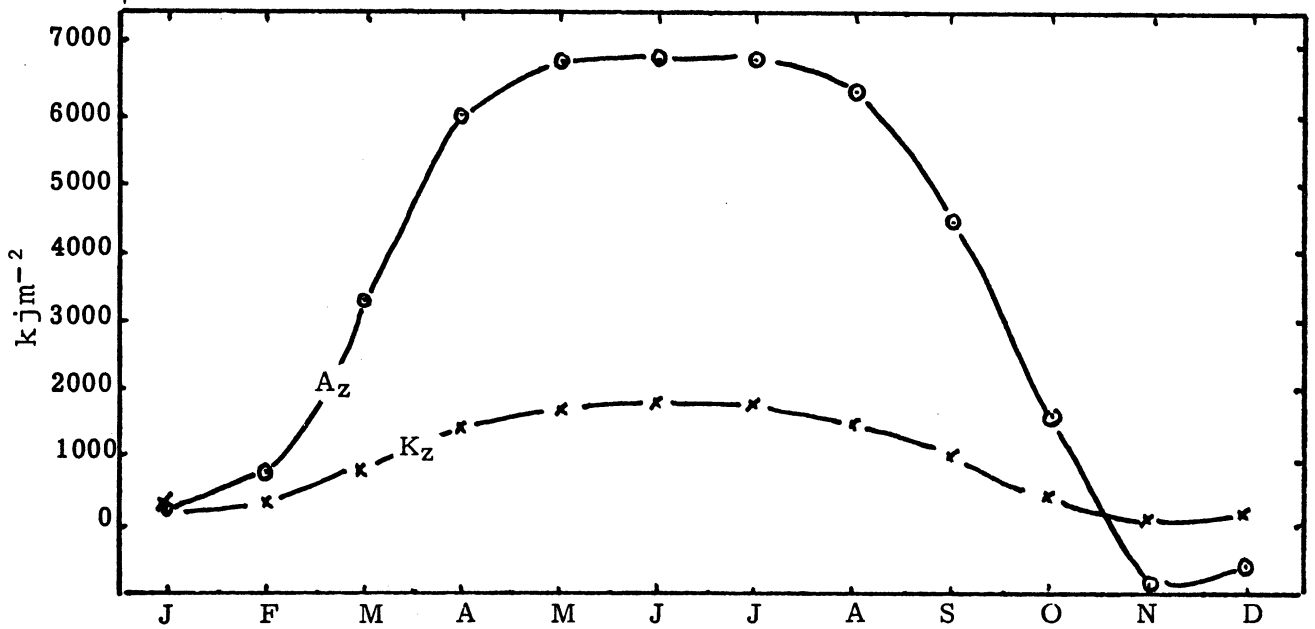
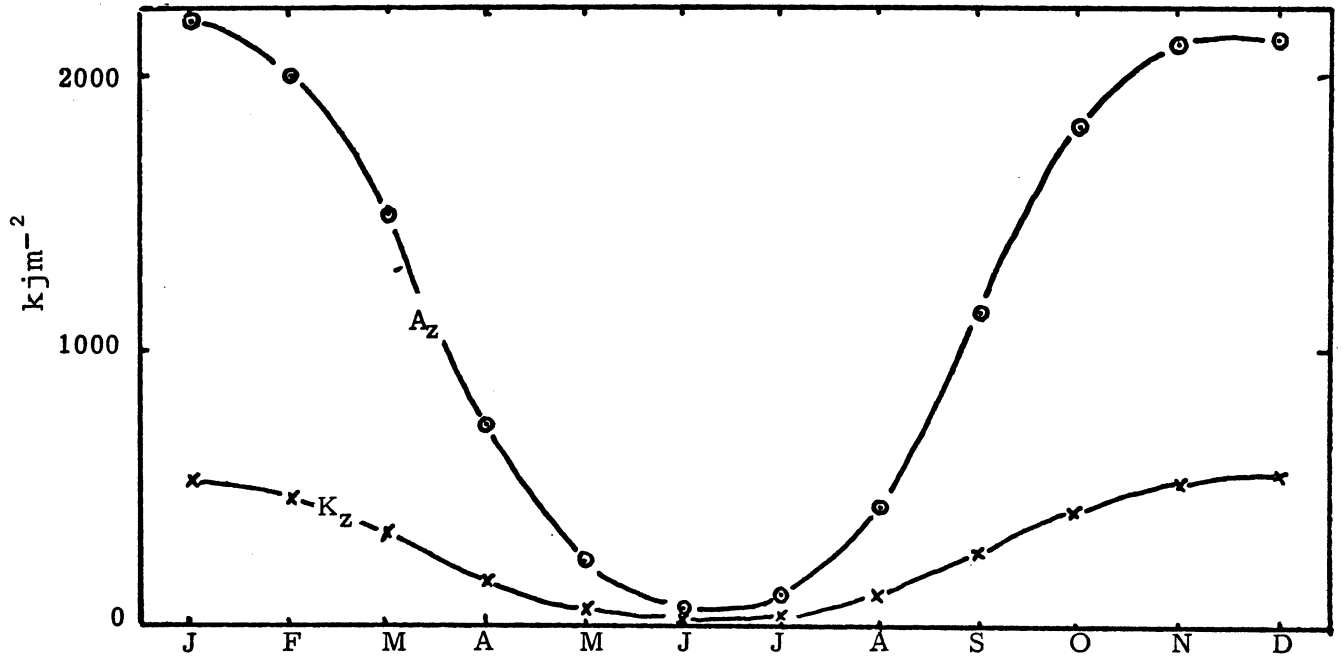


Figure 17: As Fig.7, but for Exp.No.1

the annual variation of A_z is much larger than found from observational studies. The winter maximum is about 8000 kJm^{-2} in the northern hemisphere as compared with about 5600 kJm^{-2} in the recent estimate by Peixoto and Oort (1974). On the other hand, the minimum during the summer season is much lower in the experiment than in the real atmosphere. Similar remarks can be made for K_z . For both quantities it is found that the minimum during summer is very flat with a tendency for a small secondary maximum. This is strongly connected with the temperature distribution in the summer months in the first experiments and the resulting easterlies which are found at both levels. The annual variations of A_z and K_z in the second experiment are shown for the two hemispheres in Figure 18. The amounts are now greatly reduced and are as a matter of fact below the values based on observations.

Figures 19 and 20 show finally the generation of zonal available potential energy $G(A_z)$ in the two experiments. The generation is of relative small magnitude, but stays positive throughout the year. In both calculations there is a definite tendency for a maximum during the fall with another maximum some time after the winter solstice. There is needless to say very significant differences between these results and those obtained from observational studies. Particularly, it should be noted that the secondary maximum in the later part of the winter is found at a time when Oort and Peixoto (1974) find a minimum, even negative values, in some estimates.

Northern Hemisphere



Southern Hemisphere

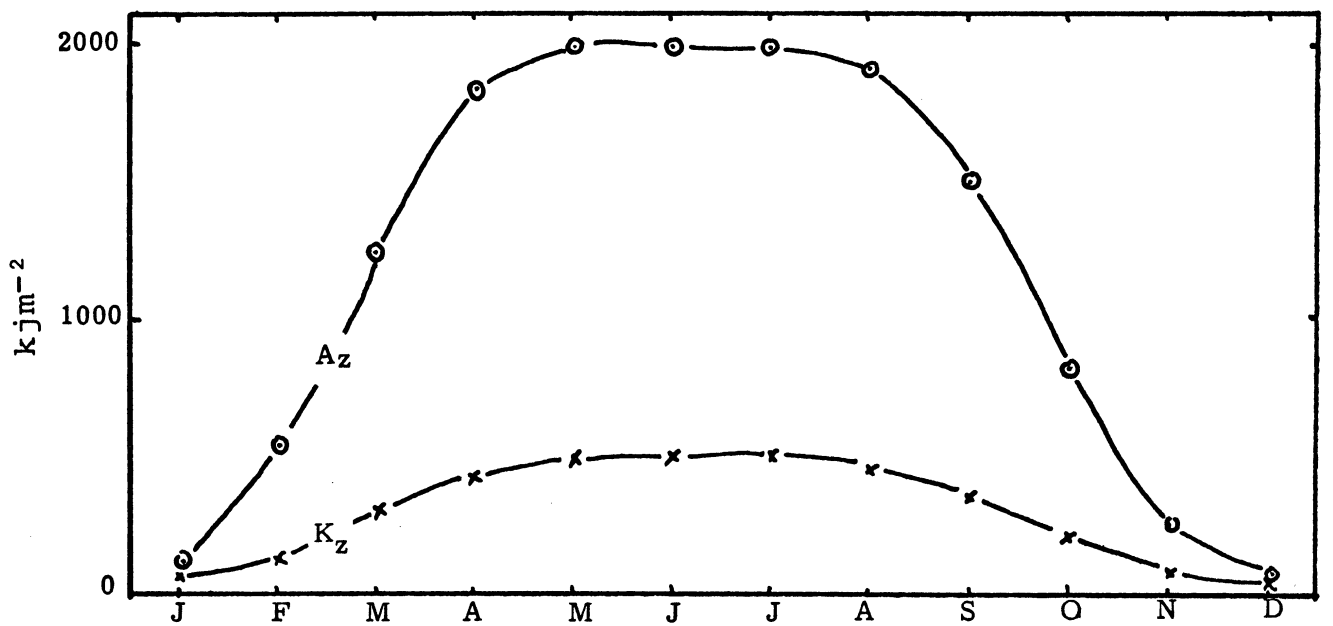
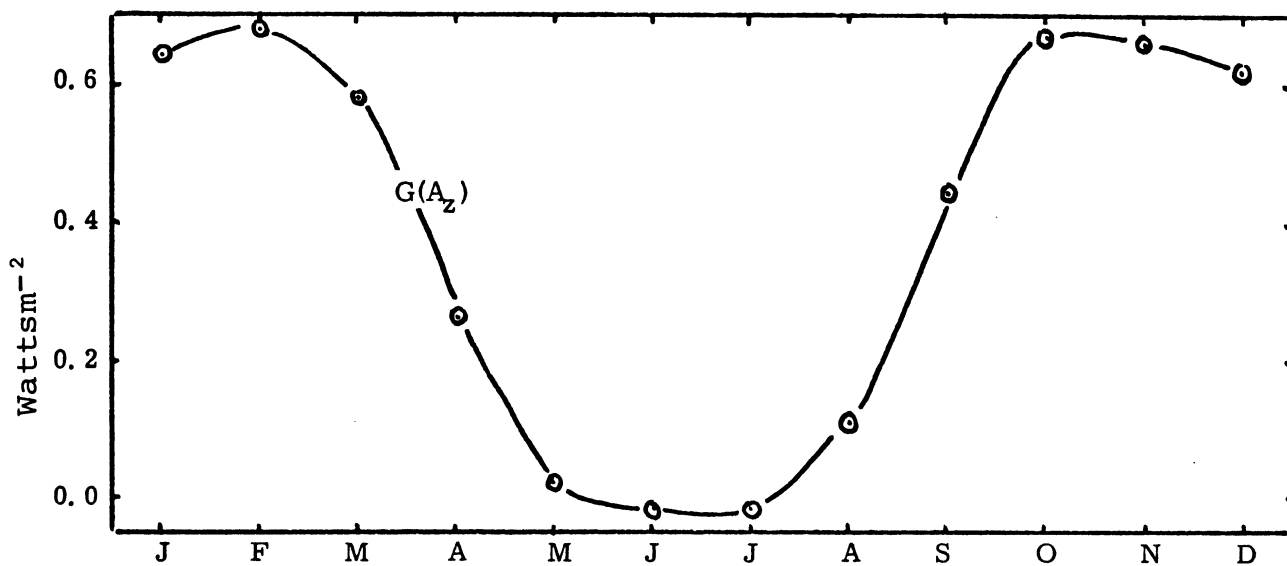


Figure 18: As Fig.7, but for Exp.No.2.

Northern Hemisphere



Southern Hemisphere

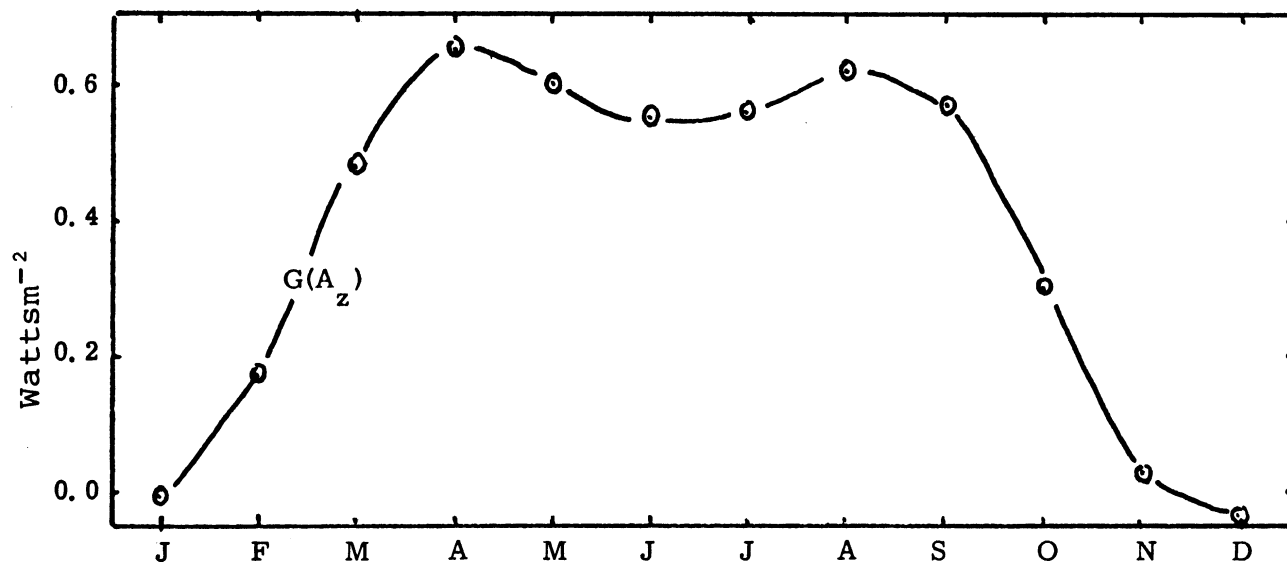
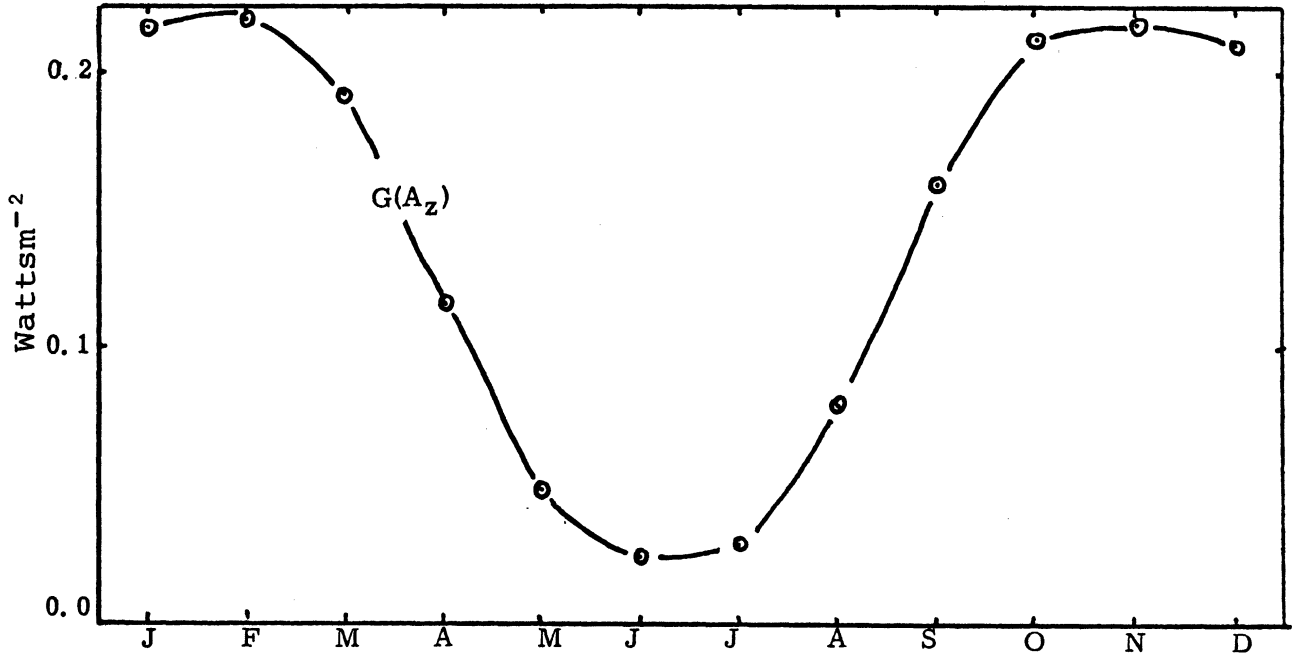


Figure 19: As Fig.8, but for Exp.No.1.

Northern Hemisphere



Southern Hemisphere

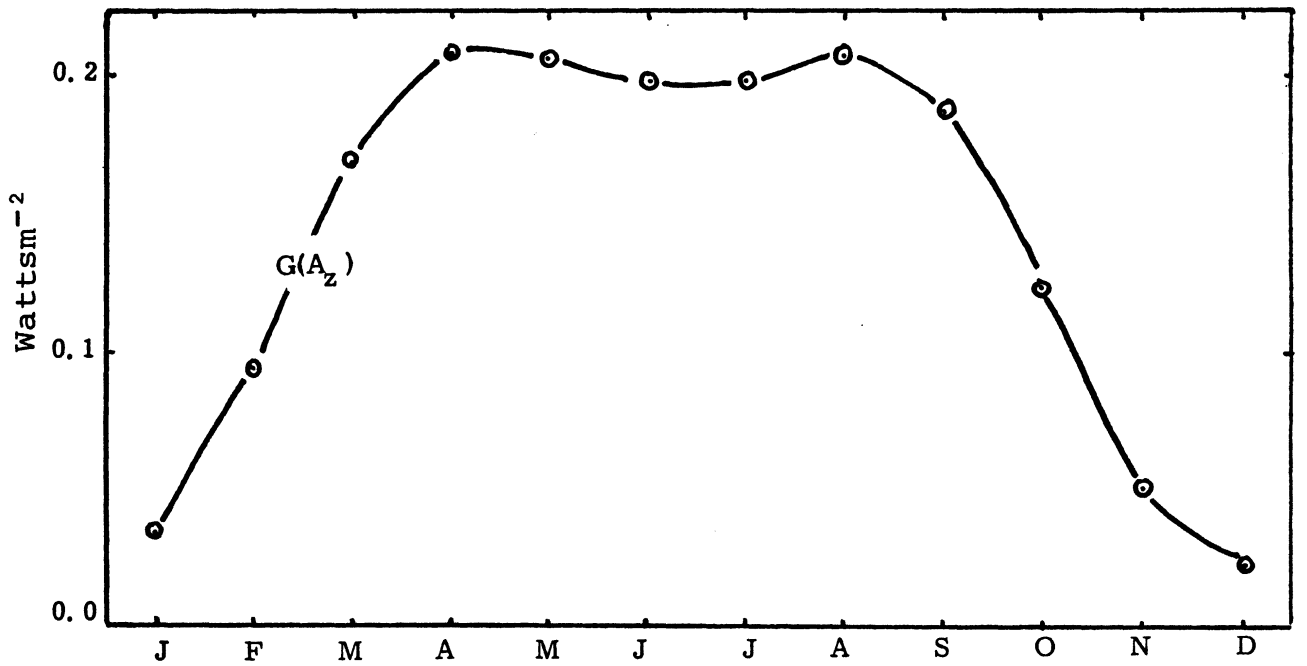


Figure 20: As Fig.8, but for Exp.No.2.

5. CONCLUDING REMARKS

The purpose of this paper has been to provide a calculation of the temperature, wind and vertical velocity distributions in an axially symmetric, steady state model of the quasi-geostrophic, two level type. The model excludes particularly the influence of the atmospheric eddies on the zonally average parameters of the model. It has naturally been known for a considerable number of years that the large-scale eddies in the atmosphere are very significant in transporting heat, moisture and momentum, and that these transports in turn influence the zonally averaged fields to a significant degree. It is therefore obvious that the present calculations are not presented as an attempt to provide a realistic model of the zonally averaged state of the atmosphere because such a model must at least include the effects of the eddies in a parameterized form as has been attempted by Fuenzalida (1973) and Wiin-Nielsen and Fuenzalida (1974). However, in order to fully appreciate the thermodynamics and the dynamics of the zonally averaged state of the atmosphere it is of interest to estimate what the atmospheric structure in the meridional plane would be if no eddies were present. The present paper is an attempt to provide a relatively simple estimate of the axially symmetric structure (temperature, wind, etc.) as determined by a given heating field and a specified dissipation.

As has been discussed in detail by Lorenz (1967) such an attempt is by no means straightforward. One of the major

difficulties is naturally the modelling of the heating mechanism. In section 3 of this paper we have adopted a specified heating field determined from a given model of the atmospheric heat budget. This model makes use of climatological information about the atmosphere and the upper layer of the ocean. One may indeed say that such a diagnostic calculation of heating is determined to a very large degree by the real atmosphere, its temperature and wind fields, and that it therefore is the heating which exists when the atmosphere contains eddies. In spite of this serious limitation it is nevertheless of interest to see what the axially symmetric, steady state would be because it adds very much to the interpretation of the corresponding calculations when the steady state assumption is removed and the effects of the eddies are parameterized. Interpreted in this way the results in section 3 supplements the results presented by Wiin-Nielsen and Fuenzalida (1974) because the difference between the two sets of results clearly shows how important it is to model the heat and momentum transport by eddies in a correct manner and the necessity to consider the annual variation of atmospheric circulations as a time-dependent problem.

6. ACKNOWLEDGMENTS

The research leading to this paper has been supported by the National Science Foundation under Grant GA-16166. The authors wish to thank Dr. James Pfaendtner for valuable programming assistance.

REFERENCES

- Derome, J., and A. Wiin-Nielsen, 1971: The response of a middle-latitude model atmosphere to forcing by topography and stationary heat sources, *Monthly Weather Review*, Vol. 99, pp. 564-576.
- Derome, J. and A. Wiin-Nielsen, 1972: On the maintenance of the axisymmetric part of the flow in the atmosphere, *Pure and Applied Geophysics*, Vol. 95 - III, pp. 163-185.
- Fuenzalida, H. A., 1973: On the simulation of the axisymmetric circulation of the atmosphere, Technical Report, University of Michigan, 002630-9-T, 190 pp.
- Lawniczak, G. E., 1969: On a multi-layer analysis of atmospheric diabatic processes and the generation of available potential energy, Technical Report, University of Michigan, 08759-5-T, 111 pp.
- Lawniczak, G. E., 1970: Additional results from multi-layer calculations of atmospheric diabatic processes and the generation of available potential energy, Technical Report, University of Michigan, 002630-2-T, 71 pp.
- Lorenz, E. N., 1967: The nature and theory of the general circulation of the atmosphere, World Meteorological Organization, 161 pp.
- Oort, A. H. and J. P. Peizoto, 1974: The annual cycle of the energetics of the atmosphere on a planetary scale, *Journal of Geophysical Research*, Vol. 79, No. 18, pp. 2705-2719.

- Wiin-Nielsen, A., 1970: A theoretical study of the annual variation of atmospheric energy, *Tellus*, Vol. 22, pp. 1-16.
- Wiin-Nielsen, A., 1972: Simulations of the annual variation of the zonally-averaged state of the atmosphere, *Geophysica Norwegica*, Vol. 28, No. 6, pp. 1-45.
- Wiin-Nielsen, A. and H. A. Fuenzalida, 1974: On the simulation of the axisymmetric circulation of the atmosphere, submitted for publication in *Tellus*.

UNIVERSITY OF MICHIGAN



3 9015 03483 0656